Science of the Total Environment 990 (2025) 179845

Contents lists available at ScienceDirect

Science of the Total Environment

journal homepage: www.elsevier.com/locate/scitotenv

Phenotypic plasticity in Mediterranean gorgonians *Eunicella singularis* and *Paramuricea clavata* at high temperature and low pH

Murat Belivermiş [a,*], Önder Kılıç [a], H. Barış Özalp [b,c], Selcan Demiralp [d], Selda Gezginci-Oktayoglu [a], Vahap Eldem [a], Berna Şahin [d], Mehmet Ali Balcı [d], Selahattin Barış Çay [d], Onur Gönülal [e]

[a] Department of Biology, Faculty of Science, Istanbul University, Istanbul, Türkiye
[b] Underwater Technology Section, Maritime Vocational School, Çanakkale Onsekiz Mart University, Çanakkale, Türkiye
[c] Water Quality Lab, Faculty of Marine Science and Technology, Çanakkale Onsekiz Mart University, Çanakkale, Türkiye
[d] Institute of Graduate Studies in Sciences, Istanbul University, Istanbul, Türkiye
[e] Department of Marine and Freshwater Resources Management, Faculty of Aquatic Sciences, Istanbul University, Istanbul, Türkiye

HIGHLIGHTS

- The oxygen consumption of the gorgonian corals increased at high temperatures.
- Energy reserves were not affected by high temperature, low pH or their interaction.
- The global DNA methylation in *Eunicella singularis* was not affected by high temperature, low pH, or their combination.
- Global DNA methylation in *Paramuricea clavata* decreased under high temperature and low pH.
- High temperature alone caused more DEGs in *E. singularis* than low pH or combined treatment.

GRAPHICAL ABSTRACT

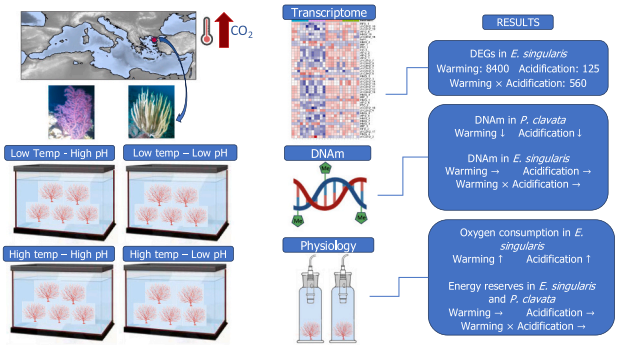

ARTICLE INFO

Editor: Julian Blasco

Keywords:
Warming
Acidification
Coral
Physiology
Transcriptome
DNA methylation

ABSTRACT

The Mediterranean gorgonian octocorals are threatened by acidification, warming and marine heat waves. Phenotypic plasticity is critical for slow-growing gorgonians, as adaptation through natural selection might not be fast enough to cope with rapid environmental changes. DNA methylation (DNAm) is a type of (trans) generational phenotypic plasticity mechanism that may help slow-growing corals better withstand the effects of environmental changes by adjusting gene expression. This study aimed to assess the physiological responses and epigenetic modifications associated with phenotypic plasticity in the Mediterranean gorgonians *Eunicella singularis* and *Paramuricea clavata* exposed to warming (+4 °C), acidification (−0.35 pH_T units) and their combination over two weeks. In addition, RNA-Seq-based differential gene expression analysis was performed for *E. singularis*.

High temperature, low pH and their combination did not cause tissue death or necrosis in the corals. Polyp activity in *E. singularis* increased at high temperatures. Warming increased oxygen consumption in both species. Energy reserves (protein, lipid, carbohydrate contents) were not affected by temperature, pH or their interaction

* Corresponding author.
E-mail address: belmurat@istanbul.edu.tr (M. Belivermiş).

https://doi.org/10.1016/j.scitotenv.2025.179845
Received 11 December 2024; Received in revised form 17 May 2025; Accepted 4 June 2025
0048-9697/© 2025 Elsevier B.V. All rights are reserved, including those for text and data mining, AI training, and similar technologies.

in either species. The global DNA methylation (gDNAm) rate was ten times higher in *P. clavata* than in *E. singularis*. There was no effect of temperature, pH or their interaction on gDNAm in *E. singularis*. gDNAm in *P. clavata* decreased at high temperatures and low pH. Differential gene expression analysis indicated that high temperature induced the most extensive transcriptional changes in *E. singularis*, while low pH alone had the least impact. The combined stress of high temperature and low pH also led to notable up- and downregulation of gene expression. Heat stress in *E. singularis* caused widespread downregulation of transcription factors (TFs), particularly those in the *zf-C2H2*, *AP-2*, and *HMG* families. Conversely, the *IRF*, *RFX*, *P53*, and *NRF1* families were upregulated, highlighting the complex transcriptional response to thermal stress. Overall, these physiological, transcriptomic and epigenetic alterations have the potential to negatively impact the fitness of these emblematic species and their associated ecosystems.

1. Introduction

The Mediterranean Sea is warming more rapidly than the ocean average (MEDECC, 2024; Garrabou et al., 2022). For example, there has been evidence of a 1.6 °C rise in sea surface temperature in the Northeast Aegean Sea over the past forty years (Gönülal, 2021). Mass mortality events (MMEs) have progressively increased in the Mediterranean Sea, which has been attributed to a steady increase in the frequency and intensity of marine heat waves (MHWs) (Rivetti et al., 2014; Garrabou et al., 2022; Estaque et al., 2023; Diaz-Almela et al., 2007). Coralligenous habitats are among the most affected by MHWs in the Mediterranean Sea (Gómez-Gras et al., 2022; Orenes-Salazar et al., 2023; Garrabou et al., 2022). A temperature increase to the upper limit of the thermotolerance window during MHWs causes (sub)lethal damage in gorgonian corals. Besides warming, elevated CO_2 in surface seawater results in an increase in seawater H^+ ion concentration, and other changes in carbonate chemistry (Feely et al., 2010; Doney et al., 2012). Consequently, since the start of the Industrial Revolution, the average H^+ ion concentration of surface seawater has increased by approximately 30 %. Projected values of pH in the context of ocean acidification (OA) in coastal zones significantly deviate from levels that are projected for the open ocean (Feely et al., 2010; Cai et al., 2011; Melzner et al., 2013). Highly productive coastal areas naturally experience wide diurnal swings in pH as photosynthesis and respiration peak at different times of day. The biological reaction is affected by this, since certain species might become regionally acclimated to this high degree of fluctuation and subsequently withstand low pH levels (Vargas et al., 2017, 2022). There is overwhelming evidence that OA has significant impacts on marine species and ecosystems (e.g., Barton et al., 2012; Dupont et al., 2013; Cole et al., 2016; Dahlke et al., 2017; Rosa et al., 2017; IPCC, 2022; Belivermiş et al., 2020, 2023). Considering the effects of OA on calcification/growth, photosynthetic rates, and internal pH regulation in marine organisms, corals are the second most negatively affected taxon following coralline algae, with a tipping point at a seawater pCO_2 of 500–900 μatm (Cornwall et al., 2023). Under the Representative Concentration Pathway 8.5 (RCP8.5) scenario, a high greenhouse gas concentration trajectory adopted by the Intergovernmental Panel on Climate Change (IPCC), coral calcification rates are projected to decline significantly by 2050 due to OA (e.g., $pCO_2 \approx 572$ μatm) (Cornwall et al., 2021).

The habitat-forming emblematic octocorals of the Mediterranean Sea display some physiological alterations under high temperatures, such as a range of 22–25 °C, which is 3–4 °C higher than their optimum temperature ranges. The negative impacts of the thermal stress have been demonstrated in Mediterranean gorgonian octocorals, such as reduced polyp activity and respiration in *Corallium rubrum*, *Eunicella cavolini*, *Eunicella singularis*, and *Paramuricea clavata* (Previati et al., 2010), the induction of the antioxidant defenses and *HSP70* in *E. singularis* (Pey et al., 2011), the loss of energy reserves and reduced feeding ability in *P. clavata* and *E. cavolini* (Tignat-Perrier et al., 2022), and decreased respiration and photosynthesis in *E. singularis* (Ezzat et al., 2013). At 25 °C and above, tissue necrosis and mortality have been reported, which are exacerbated with a longer exposure period (Previati et al., 2010; Pivotto et al., 2015; Crisci et al., 2017; Gómez-Gras et al., 2022). Some studies have shown that various populations of gorgonian species living in different seas in the Mediterranean Sea present very similar thermotolerance phenotypes. This could be explained by genetic drift other than local adaptation (Crisci et al., 2017; Gómez-Gras et al., 2022).

The relationship between acidification and gorgonian physiology has not received as much attention as that between warming and gorgonian physiology. A decrease in the skeletal growth rate was shown in the Mediterranean gorgonian coral *Corallium rubrum* under low pH conditions (Bramanti et al., 2013). In another study, elevated pCO_2 (700 μatm), alone or in combination with elevated temperature, did not affect photosynthesis or calcification rates in the Mediterranean scleractinian coral *Cladocora caespitosa* (Rodolfo-Metalpa et al., 2010). However, the negative effects of low pH on scleractinian corals have been well documented worldwide (see Leung et al., 2022).

The current rate of climate change may outweigh marine metazoans' ability to adapt to future conditions (Liew et al., 2018; Aranda Lastra, 2022). Epigenetic mechanisms such as DNAm in scleractinian corals could offer them a greater ability to buffer the impacts of environmental changes such as warming and acidification by fine-tuning gene expression (Putnam et al., 2016; Putnam, 2021; Liew et al., 2018; Dimond and Roberts, 2016; Aranda Lastra, 2022). Moreover, gene body DNA methylation differs between housekeeping and environmentally responsive genes, which aids acclimatisation, as demonstrated in the reef-building coral *Acropora millepora* (Dixon et al., 2018). Liew et al. (2018) reported a significant increase in gDNAm in the reef-building coral *Stylophora pistillata* with decreasing pH.

Phenotypic plasticity is critical for metazoans with long generation times, such as slow-growing gorgonians, as adaptation through natural selection might not be fast enough to cope with rapid environmental changes. However, under environmental changes, epigenetic mechanisms such as the effects of DNAm on phenotypic plasticity have remained unresolved in gorgonians. The gorgonian corals *Eunicella singularis* and *Paramuricea clavata* are the species most affected by warming and MHWs in Mediterranean rocky benthic communities (Garrabou et al., 2009, 2022; Iborra et al., 2022; Orenes-Salazar et al., 2023). Although the physiological effects of high temperatures on gorgonians have been documented (Previati et al., 2010; Pivotto et al., 2015; Crisci et al., 2017; Gómez-Gras et al., 2022), the effects of exposure to a combination of warming and acidification, as well as the underlying mechanisms, remain unresolved. We postulated that the transcriptomic pattern and epigenetic modifications would shape the phenotypic plasticity of gorgonians under high temperatures and low pH. This work aims to evaluate gorgonians' physiological responses such as polyp activity, oxygen consumption and energy reserves (protein, lipid and carbohydrate contents) to warming, acidification and their combination over two weeks, as well as to understand the underlying epigenetic and transcriptomic mechanisms of their phenotypic plasticity. These endpoints provide a holistic view of how high temperatures and low pH affect physiology, DNAm and gene expression profiles.

2. Materials and methods

2.1. Site surveys and coral sampling process

The Çanakkale Strait, also known as the Dardanelles in former times, represents one of the species-rich habitats of marine invertebrates in the Turkish seas. The Mediterranean-originating deep water and upper-level mixing surface water, involving two different characteristics, the Black Sea and the Marmara Sea, with continuous dominant tides, enable a special biodiversity status in the area (Özalp and Alparslan, 2016) (Fig. 1). Among these species-rich sites, some coral species, such as *Eunicella singularis*, *Eunicella cavolini*, *Cladocora caespitosa*, *Paramuricea clavata* and *Savalia savaglia*, form structural facies that support marine animal feeding, breeding, and sheltering needs in the environment. During site surveys, the highest abundance of *E. singularis* was observed in 65 colonies (8 with severe necrosis), whereas there were over 1000 healthy colonies of *P. clavata* within the station examined (Fig. 1: blue-marked area on the map).

A sampling process was performed by the scientific diving team of COMU (Çanakkale Onsekiz Mart University). White gorgonian coral (*E. singularis*) colonies were sampled at upper and lower depth limits of 12–23 m. The largest area of both species has been found in the southern regions of the strait (European side) (Fig. 1: blue-marked station on the map, Baykuşfener-Kilitbahir). The temperature and salinity at the sampling depth were measured as 14 °C and 37 ppt, respectively. Following the completion of the *E. singularis* experiment, colony samples of the Mediterranean red gorgonian *P. clavata* were obtained from the exact station by scientific divers at a depth of 35–37 m from the rocky zone on the European side of the Çanakkale Strait. During the sampling process, a fragment of approximately 20 × 15 cm was cut with stainless-steel underwater scissors from ten and seven colonies of *E. singularis* and *P. clavata*, respectively (Fig. S1). Following their transfer into the boat, the corals were placed inside 3-L plastic bottles with perforated lids. The bottles were placed in a cooler with a controlled temperature to match the location of the sampling. Within 5 h, the corals were transported from the sample location to the laboratory.

From the first day in the laboratory, corals were maintained in ASW (artificial seawater) at 16–18 °C. Then they gradually acclimated to 20 °C within three days. On the fourth day in the laboratory, gorgonian tips (5–7 cm, referred to as fragments hereafter) were cut from the colonies and glued on a silicon stopper using nontoxic coral adhesive glue (Aquaforest Gel Fix). Consequently, 120 and 84 fragments were obtained from *E. singularis* and *P. clavata* colonies, respectively (Fig. S1). They were allocated to 12 glass aquariums: ten and seven fragments at each aquarium for *E. singularis* and *P. clavata*, respectively. Each aquarium consisted of one fragment from each colony. From the day the coral fragments were allocated to the aquariums, a one-week acclimation period began under ambient conditions, i.e., 20 °C and pH: 8.00.

The aquariums were filled with 12 L of ASW, which was prepared using sea salt (Instant Ocean) and distilled water for a final salinity of 37. The seawater was renewed daily, and the corals were fed live *Artemia salina* nauplii (1000 nauplii L^{-1}) three times a week. A high flow rate (300 L h^{-1}) was provided in the aquariums via submersible circulation pumps (Eheim compactON 300, Germany). After a three-day dark period, the illumination of the aquarium was changed to a day/night cycle (12 h of light and 12 h of dark). A combination of two T5 lamps was used for illumination (Solar Marine Day Ultra 15,000 K and Solar Nature Ultra 9000 K, JBL, Germany). The light intensity was adjusted considering the depth and water turbidity where corals were collected. The light intensity (photosynthetically active radiation) reaching the corals was measured in the aquariums with an underwater quantum meter (Apogee MQ-210X, USA), and the average value was 35 ± 5 µmol m^2 s^{-1}.

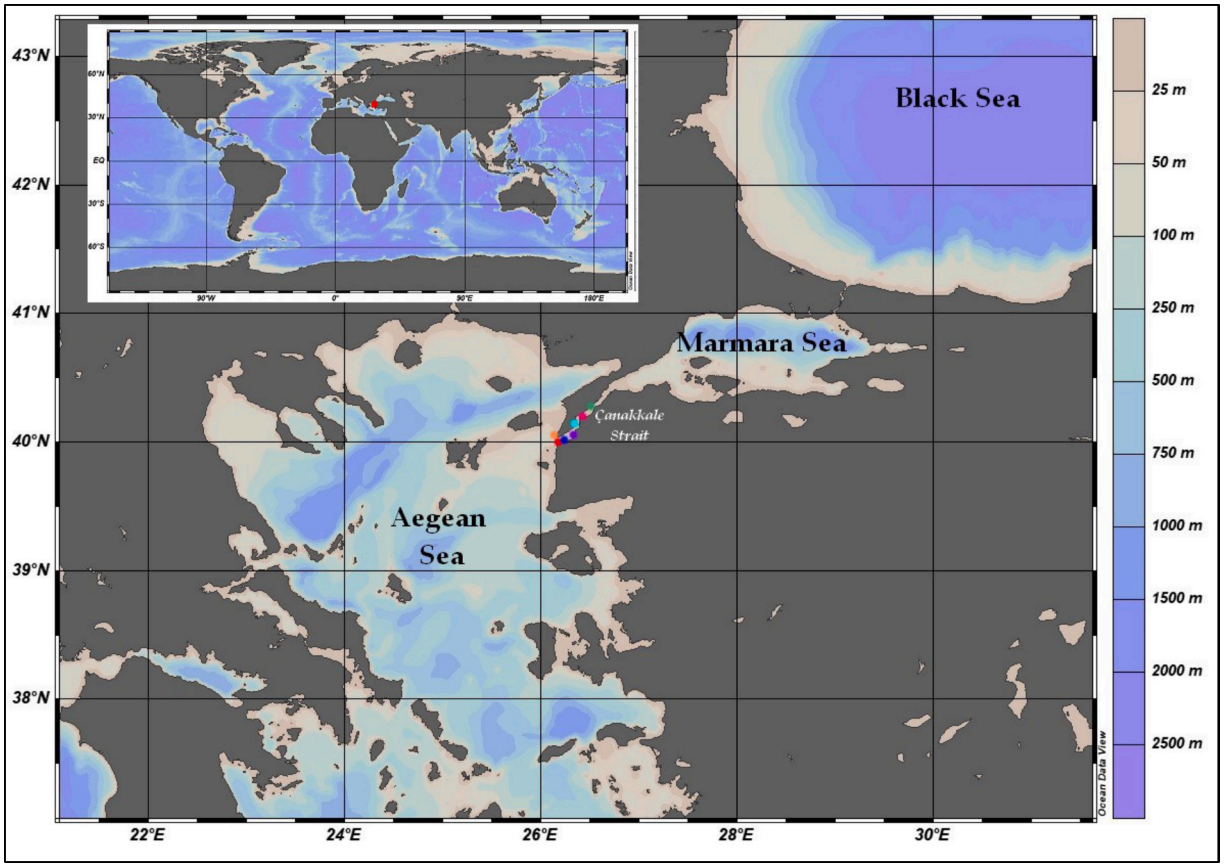

Fig. 1. Survey sites in the Çanakkale Strait (the Dardanelles).

2.2. Temperature and pH manipulation

The pH and temperature of the seawater were measured via an aquarium conditioning device (IKS Aquastar, Germany) at sensitivities of 0.01 pH units and 0.1 °C, respectively. Lowering the pH was achieved by slowly bubbling pure CO_2 into seawater. Before each seawater renewal, the pH and temperature in each treatment aquarium were adjusted to their respective target values. The dissolved oxygen level ranged from 7.0 to 7.5 mg L^{-1}. Three aquariums were used for each treatment (3 replicates × 4 treatments = 12 aquariums). A full cross-breeding design was used, leading to four different treatments replicated three times: (i) low temperature/high pH (T:20 °C, pH:8.00), (ii) low temperature/low pH (T:20 °C, pH:7.65), (iii) high temperature/high pH (T:24 °C, pH:8.00), and (iv) high temperature/low pH (T:24 °C, pH:7.65) (Fig. S2: Experimental set-up). Low temperature/high pH (T:20 °C, pH:8.00) treatment reflects ambient conditions. Thermostat heaters (Eheim Thermocontrol E20, Germany) were used to warm the seawater in the high-temperature aquariums.

For temperature, the two tested levels were (i) 20 °C, within the present range of variability and, (ii) 24 °C, outside the present range of variability and relevant in the context of warming and MHWs (IPCC, 2021; MEDECC, 2024). Following a one-week acclimation period under ambient conditions, i.e., 20 °C, the temperature in six of the aquariums gradually increased to 24 °C within 24 h. Two pH scenarios were selected for this study: (i) $pH_T = 8.00$, corresponding to the pH at the sampling site at the time of collection and well within the present range of variability, and (ii) $pH_T = 7.65$, which is at the extreme of the present range of variability, and is relevant in the context of ocean acidification. Select low pH (7.65) is relevant in the context of high and very high greenhouse gases emission scenarios (SSP3–7.0 and SSP5–8.5) (IPCC, 2021). Accordingly, the pH_{NBS} levels in the six low-pH aquariums progressively decreased by 0.35 pH units over a day. pH values on the total scale (pH_T) were measured every week via a pH meter (Metrohm 913) and calibrated with Tris/HCl buffer solution provided by the Marine Physical Laboratory at the Scripps Institution of Oceanography (Dickson et al., 2007). The target temperature and pH_T values of the experiment (temperature: 20 vs. 24 °C; pH_T: 8.00 vs. 7.65) were successfully maintained throughout the exposure (Table S1). For both species, we confirmed that (i) the establishment of two separate temperature and pH treatments and (ii) temperature did not differ among low-temperature replicate aquariums and among high-temperature replicate aquariums. pH did not differ among high-pH replicate aquariums. pH differed among low-pH replicate aquariums in *E. singularis*, among low-pH replicate aquariums and among high-pH replicate aquariums in *P. clavata* (Table S2).

2.3. Polyp activity and oxygen consumption

The ratio of open polyps to all polyps served as the basis for evaluating polyp activity. Either partially or totally enlarged polyps were classified as open polyps. Based on the number of open polyps to the total number of polyps, a score was assigned between 0 and 5 for each fragment.

The oxygen consumption rate (OCR) was measured at the end of two weeks of exposure as detailed in previous studies (Belivermiş et al., 2023; Gammon et al., 2018; Previati et al., 2010). Three *E. singularis* fragments were taken from each aquarium (nine fragments per treatment). Seven *P. clavata* fragments per treatment were taken from the aquariums. Then, a total of 36 *E. singularis* and 28 *P. clavata* fragments were placed in an airtight 330 mL respiration chambers. The dissolved oxygen (DO) concentrations were measured with optic oxygen probes (IKS Aquastar ODOS, Germany) attached to a flow-through cell. After 15 min of placing the coral fragments, the DO values were recorded as the initial DO concentration (C_{t0}). Three hours later, the DO level was recorded again (C_{t1}). Since *E. singularis* is a symbiotic species, the test was carried out in the dark to cease symbiodinium photosynthesis. During each measurement, one chamber without a coral fragment was used as a blank. The DO values of the blank chambers were subtracted from those measured in the coral chamber. Following the completion of the oxygen consumption test, the axial skeleton of the corals was discarded, and the fresh weights (coenenchyma and polyps) were determined.

The OCRs were determined on the basis of the ash-free dry weight (AFDW), which was calculated from the organic matter loss of the tissues at 450 °C. First, 20 mg of coral tissue (coenenchyma and polyps, no axis) was freeze-dried to determine the dry weight. The dry tissue was subsequently heated to 450 °C in an ash oven for 4 h. The difference between the ash and dry weight provided AFDW (Rossi et al., 2006).

The oxygen consumption rate was then calculated as follows:

$$OCR = \frac{[(C_{t0} - C_{t1}) \times V]}{t \times AFDW}$$

where OCR is the oxygen consumption rate in per gram of AFDW coral tissue (mg O_2 h^{-1} g $AFDW^{-1}$); C_{t0} and C_{t1} are the DO concentrations (mg O_2 L^{-1}) at the beginning and end of the test, respectively; V (L) is the water volume in the respiration chamber; and t (h) is the test time.

2.4. Global DNA methylation

At the end of the exposure, approximately 250 mg of coral tissue (coenenchyma and polyps) was taken from three coral fragments in each aquarium (9 per treatment). The samples were flash-frozen in liquid nitrogen and kept at −80 °C until analysis. For *E. singularis*, 100 mg of wet tissue was homogenised (2 cycles at 7000 rpm for 40 s; Magna Lyser, Roche) via homogenisation buffers and beads from a DNA isolation kit (Quick-DNA Plant/Seed Miniprep Kit, Zymo). Genomic DNA was extracted from *E. singularis* tissues via a kit. The salting-out protocol was used for extracting DNA from *P. clavata* tissues (Macleod et al., 2023). Thirty milligrams of tissue (7 per treatment) was homogenised in a tissue homogeniser (2 cycles at 7000 rpm for 40 s; Magna Lyser, Roche). The amount and purity of the DNA were measured with a Nanodrop instrument (BioSpec-nano-Shimadzu). The gDNAm of the corals was assessed colourimetrically in duplicate using a methylated DNA immunoprecipitation assay according to the manufacturer's instructions (MethylFlash Methylated DNA Quantification Kit, P-1034, Epigentek) and reported as % methylated DNA, relative to the input DNA quantity for each coral sample. The ratio of 5-mC nucleotides to all nucleotides was given as the proportion of methylated DNA.

2.5. Energy reserves

At the end of the experiment, the coral tissues (coenenchyma and polyps) were separated from the central proteinaceous axis and analysed for energy reserves (carbohydrate, protein, lipid) content. The tissues were individually analysed for each treatment ($n = 9$ for *E. singularis*, $n = 7$ for *P. clavata*).

Proteins were extracted from 4 mg of freeze-dried tissue in 150 μL of 1 M NaOH at 90 °C for 30 min (Tignat-Perrier et al., 2022). The samples were subsequently centrifuged at 3000 ×*g* for 4 min at 4 °C. The supernatant was used to quantify the soluble protein concentration. BCA protein assay kit (BioBasic, Canada) was used following the manufacturer's instructions. For carbohydrates, 15 mg of dry tissue was homogenised in 350 μL of 0.1 % Triton by using a tissue homogeniser (2 cycles at 7000 rpm for 40 s; Magna Lyser, Roche). The samples were subsequently centrifuged at 3000 ×*g* for 4 min at 4 °C twice to obtain a clear homogenate. The phenol-sulfuric acid method was applied to measure carbohydrate concentrations in homogenates (Masuko et al., 2005). A total of 600 μL of concentrated H_2SO_4 and 120 μL of 5 % phenol were added to 200 μL of the sample or glucose standard. The samples were incubated at 90 °C for 5 min in a heating block and then cooled. The absorbances of carbohydrates and protein were read at 492 and 562 nm,

respectively, using a microplate reader (Biotek).

The colorimetric sulfo-phospho-vanillin method was used to determine the total lipid content (Van Handel, 1985; Falfushynska et al., 2019). The pellet remaining from the DNA extraction procedure of *E. singularis* was diluted and centrifuged at 3000 ×*g* for 6 min at 4 °C. The supernatant was used for lipid measurement. For *P. clavata*, 30 mg of tissue was homogenised in a tissue homogeniser (2 cycles at 7000 rpm for 40 s; Magna Lyser, Roche) using a mixture of chloroform-methanol (1:1 in volume) and ceramic beads. A total of 250 μL of extracted lipids or soybean oil standards was dried at 100 °C for 10 min in a heating block to evaporate the chloroform and methanol. Then, 100 μL of concentrated H_2SO_4 was added to each sample and heated airtightly at 100 °C for 10 min. The sample was cooled to room temperature, mixed with 2.4 mL of vanillin reagent (600 mg vanillin in 100 mL of hot water mixed with 400 mL of 85 % phosphoric acid) and incubated for 5 min. The absorbances were read at 490 nm using a microplate reader (Biotek). Protein, carbohydrate and lipid contents were determined based on ash-free dry weight (AFDW).

2.6. Transcriptome sequencing, assembly and annotation of E. singularis under experimental conditions

At the end of the exposure, coral tissue (coenenchyma and polyps) was sampled from two coral fragments per aquarium (6 per treatment). High-quality total RNA was extracted using TRIzol™ Reagent and purified with an RNeasy MinElute Cleanup Kit (Qiagen). RNA quality was assessed using NanoDrop, Qubit® Fluorometer, and Agilent Bioanalyzer 2100, with only samples having RNA Integrity Number (RIN) ≥ 7.5 selected for sequencing. Twenty-four RNA-seq libraries were prepared using the TruSeq RNA Library Prep Kit v2 (Illumina) and sequenced on the Novaseq 6000 platform (150 cycles, paired-end chemistry). The resulting data was quality-filtered and de novo assembled using Trinity v2.13.0 (Haas et al., 2013) with default parameters (k-mer size of 25, min_contig_length = 300). Assembly quality and completeness were assessed using BUSCO v5 and DOGMA against Metazoa benchmarks (Nishimura et al., 2017; Kemena et al., 2019). Redundant sequences were clustered at 98 % identity using MMseqs2 v13.45111 (Mirdita et al., 2019; Raghavan et al., 2023), and potential contaminants were removed using Kraken2 v2.1.2 (Wood et al., 2019). Functional annotation of transcripts was performed using the Trinotate pipeline v3.2.0 (Bryant et al., 2017). Protein-coding regions were identified via Transdecoder, and homology searches were conducted against UniRef90 and Pfam-A databases (UniProt, 2023). Gene families, KEGG Orthology (KO), and Gene Ontology (GO) annotations were assigned using TRAPID v2.0 webtool (http://bioinformatics.psb.ugent.be/trapid_02/) and the EggNOG 4.5.1 reference database (Bucchini et al., 2021; Cantalapiedra et al., 2021). A detailed methodology for de novo transcriptome, functional annotations and RT-qPCR analysis were given in SPM 1.

2.7. Statistical analysis

All analyses were conducted using RStudio packages (R Studio Team, 2021). The assumptions of normality and homoscedasticity of the residuals were checked via the Shapiro-Wilk test and Levene's test and visually checked via a Q-Q plot and residual vs. fits plot, respectively.

A linear model was used to assess whether temperature, pH and their interaction affect the oxygen consumption rate and carbohydrate content in *E. singularis*. A generalised linear model (gamma distribution) was used to assess whether temperature, pH and their interaction influence the protein and lipid contents in *E. singularis*. Beta distribution was used for gDNAm in *E. singularis*.

A generalised linear model (gamma distribution) was used to assess whether temperature, pH and their interaction had effects on the oxygen consumption rate in *P. clavata*. Linear models were used for carbohydrate and protein contents, whereas a generalised linear model (gamma distribution) was used for lipid contents in *P. clavata*. Beta distribution was used for gDNAm in *P. clavata*. The colony and aquarium numbers were set as random factors in the models.

Ordinal logistic regression (OLS) was used to assess whether temperature, pH and their interaction affected polyp activity in *E. singularis* and *P. clavata*. Temperature, pH and time were fixed factors, whereas colony number and aquarium number were random factors in the OLS models. Several OLS models were tested, ranging from fully interactive to fully additive. The most suitable OLS model was chosen on the basis of the Akaike information criterion (AICc).

All hypothesis testing was performed at alpha = 0.05. The partial omega squared effect size (ω_p^2), *p* value, and 95 % confidence interval of the effect size (95 % CI) were considered in each test to ascertain whether temperature, pH, time and their combination significantly affected the selected parameters.

For the transcriptome results, the gene expression values were first log-transformed. The statistical significance of the differences among groups was determined using *P* values computed by DESeq2 with generalised linear models. The P values were adjusted using the Benjamini and Hochberg method, which controls the false discovery rate to reduce the likelihood of false positive results. Genes exhibiting a fold change (log2FC > 1) with an adjusted *P*-value < 0.05 were considered differentially expressed. Next, GO and metabolic pathway enrichment were carried out using ShinyGO v0.77 web server with the following settings: 0.05 as the "P value cut-off (FDR)", and 30 as the "of most significant terms to show" (Ge et al., 2020). The Pheatmap v1.0.12 and Enhanced Volcano v1.16.0 packages (https://www.r-project.org/, R v4.3.0) were used to draw heatmaps and volcano plots, respectively, for the most significant DEGs ranked on the basis of adjusted P values.

3. Results

3.1. Polyp activity and oxygen consumption

E. singularis and *P. clavata* had overall polyp activities of 2.68 ± 1.84 and 3.33 ± 1.59 (Avg ± SD), respectively (Fig. 2). The temperature (OLS, $p = 5.1 \times 10^{-10}$, CI = 2.27 (1.55, 2.99)), but neither pH nor their interaction (OLS, $p > 0.05$) had a significant effect on polyp activity in *E. singularis* (OLS, p > 0.05) (Table 1). The polyp activity in *P. clavata* was not affected by temperature, pH or their interaction ($p > 0.05$). Polyp activity in *P. clavata* was affected by the interaction of temperature and time (OLS, $p = 0.034$, CI = −0.49 (−0.04, −0.95)) (Table 2).

The OCRs in *E. singularis* and *P. clavata* were 0.79 ± 0.55 and 0.82 ± 0.82 (Avg ± SD) mg O_2 h^{-1} g $AFDW^{-1}$, respectively (Fig. 3). The OCR of *E. singularis* was affected by temperature ($p = 0.047$, $\omega_p^2 = 0.12$) and the interaction between temperature and pH ($p = 0.012$, $\omega_p^2 = 0.20$) (Table 1).

The OCR in *P. clavata* was affected by temperature ($p = 0.029$, $\omega_p^2 = 0.08$), but not by pH or the interaction between temperature and pH (Table 2). The OCR of *P. clavata* in the high temperature/high pH treatment was much greater (by 120.4 %) than that in the low temperature/high pH treatment.

3.2. Energy reserves

In gorgonian corals, the tissue contains organic matter and sclerite ($CaCO_3$). Organic matter (AFDW) consists of soluble protein, lipids, carbohydrates, and refractory material (mainly insoluble protein) (Shirur et al., 2014; McCauley et al., 2018). The AFDW/dry tissue weight ratio (AFDW/DTW) was 0.33 ± 0.05 in *E. singularis*. The ratios of AFDW/DTW were 0.35 ± 0.03 at high temperatures/low pH, 0.32 ± 0.04 at high temperatures/high pH, 0.33 ± 0.03 at low temperature/low pH, 0.31 ± 0.07 at low temperature/high pH conditions in *E. singularis*.

The AFDW/DTW ratio was 0.25 ± 0.04 for *P. clavata*. The AFDW/DTW ratios were found to be 0.26 ± 0.03 at high temperatures/low pH, 0.23 ± 0.04 at high temperatures/high pH, 0.25 ± 0.04 at low

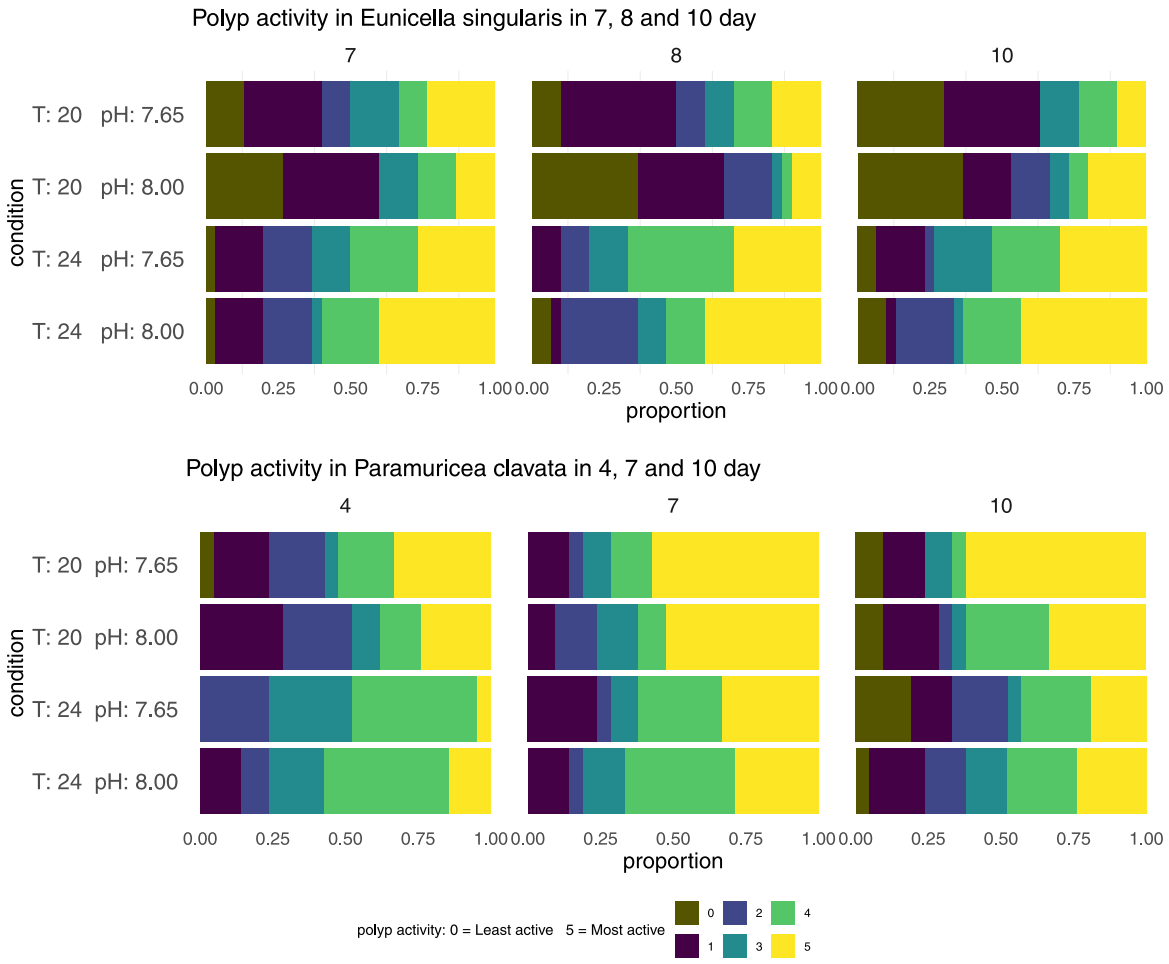

Fig. 2. Polyp activity in *E. singularis* on days 7, 8, and 10, and in *P. clavata* on days 4, 7, and 10, under exposure to four experimental conditions for two weeks: low temperature/low pH (20 °C, pH 7.65), low temperature/high pH (20 °C, pH 8.00), high temperature/low pH (24 °C, pH 7.65), and high temperature/high pH (24 °C, pH 8.00). Scores from 0 to 5, represented by different colours, indicate the percentage of open polyps relative to the total number of polyps, where 0 = least active and 5 = most active.

temperatures/low pH, 0.25 ± 0.05 at low temperatures/high pH conditions in *P. clavata*.

The energy reserves are presented in Fig. 4. The overall energy reserves were ranked as protein > lipid > carbohydrate and were very similar in *E. singularis* and *P. clavata*. The carbohydrate, protein and lipid contents in *E. singularis* were 6.25 ± 1.18, 181.4 ± 29.4, and 117.8 ± 52.0 (average ± SD, μg/mg AFDW), respectively. The carbohydrate, protein and lipid contents in *P. clavata* were 11.46 ± 2.99, 196.3 ± 46.1, and 88.8 ± 38.3 (average ± SD, μg/mg AFDW), respectively. The carbohydrate, protein and lipid contents of *E. singularis* were not affected by temperature, pH, or their interaction (Table 1). The carbohydrate, protein and lipid contents in *P. clavata* were not affected by temperature, pH or their interaction (Table 2).

3.3. gDNAm profile

Regardless of the conditions, 0.23 ± 0.15 % and 2.28 ± 2.21 % of the DNA was methylated (5mC in all nucleotides) in *E. singularis* and *P. clavata*, respectively (Fig. 5). gDNAm in *E. singularis* was not affected by temperature, pH or their interaction ($p > 0.05$) (Table 1). gDNAm in *P. clavata* was affected by temperature ($p = 0.128$, $\omega_p^2 = 0.07$), and pH ($p = 0.014$, $\omega_p^2 = 0.08$) (Table 2). Compared with individuals reared at a combination of low temperature and high pH, *P. clavata* reared at high temperature alone, low pH alone or their combination presented average gDNAm reductions of 51.9 %, 57.6 %, and 67.5 %, respectively.

3.4. Transcriptome results in E. singularis

3.4.1. Transcriptome assembly and annotation

Following the cleaning and quality check of the RNA-seq data, 24 transcriptome libraries from the four treatment groups yielded over 998.4 million clean reads, with an average of 2.75 gigabases (Gb) per sample. The results demonstrated that the Q20 value for each group exceeded 97.20 %, with an average Q30 value of 92.43 % and an average GC content of 45.57 % (Table S3). The obtained high-quality reads were de novo assembled, resulting in an *E. singularis* transcriptome comprising 54,758 genes with 144,353 transcripts covering 149.02 Mb, with an N50 value of 1.54 kb and a maximum transcript length of ~40.07 kb (Fig. 6A). Comparison of the *E. singularis* transcripts with high-quality coral transcriptomes (*P. clavata* and *Dendronephthya gigantea*) revealed a significant overlap in gene content (11,728 genes), validating the transcriptome quality and suitability for further analysis (Fig. 6B). The assessment of transcriptome completeness using the BUSCO revealed 91.19 % complete and 94.03 % complete + partial core metazoan orthologue datasets, indicating a high degree of gene content. DOGMA analysis of conserved domain arrangements (CDAs) in the *E. singularis* transcriptome revealed a completeness of 85.86 % (1652/1924), suggesting a sufficient gene repertoire (Fig. 6C and D). The functional annotations were successfully assigned to the vast majority of the predicted proteins because of the enrichment of mRNAs in the constructed Poly-A selected libraries. Among the 54,758 genes, 40,939 genes (87.32 %) and 113,979 transcripts (86.33 %) were assigned to at

Table 1
Eunicella singularis statistical test results.

Parameter	Model	Temperature	pH	Temperature × pH	Time
Oxygen consumption	General linear	**$F = 4.405$** **$p = 0.047$** **CI = 1.58 [0.60, 2.56]** **$\omega_p^2 = 0.12$**	**$F = 3.354$** **$p = 0.081$** **CI = 1.54 [0.56, 2.52]** **$\omega_p^2 = 0.09$**	**$F = 7.523$** **$p = 0.012$** **CI = −1.78 [−0.43, −3.12]** **$\omega_p^2 = 0.20$**	
Polyp activity	Ordinal logistic regression	**$Z = 6.217$** **$p = 5.1 \times 10^{-10}$** **CI = 2.27 [1.55, 2.99]**	$Z = -0.523$ $p = 0.066$ CI = 0.63 [−0.04, 1.30]	$Z = 1.661$ $p = 0.097$ CI = −0.81 [−1.77, 0.15]	$Z = -0.858$ $p = 0.391$ CI = −0.08 [−0.28, 0.11]
DNAm	Beta	$t = -1.815$ $p = 0.253$ $\omega_p^2 = 0.03$	$t = -1.013$ $p = 0.319$ $\omega_p^2 = 2.42 \times 10^{-3}$	$t = -0.246$ $p = 0.807$ $\omega_p^2 = 0.00$	
Carbohydrate	General linear	$F = 0.189$ $p = 0.666$ CI = −0.53 [−1.51, 0.45] $\omega_p^2 = 0.00$	$F = 0.090$ $p = 0.766$ CI = −0.48 [−1.46, 0.50] $\omega_p^2 = 0.00$	$F = 1.125$ $p = 0.271$ CI = 0.76 [−0.63, 2.15] $\omega_p^2 = 6.93 \times 10^{-3}$	
Protein	GLM gamma	$\chi^2 = 0.507$ $p = 0.476$ CI = −0.01 [−0.17, 0.14] $\omega_p^2 = 0.00$	$\chi^2 = 0.003$ $p = 0.953$ CI = 0.02 [−0.13, 0.18] $\omega_p^2 = 0.00$	$\chi^2 = 0.239$ $p = 0.624$ CI = −0.05 [−0.27, 0.16] $\omega_p^2 = 0.00$	
Lipid	GLM gamma	$\chi^2 = 0.033$ $p = 0.854$ CI = −0.16 [−0.56, 0.24] $\omega_p^2 = 0.00$	$\chi^2 = 0.232$ $p = 0.629$ CI = −0.20 [−0.61, 0.20] $\omega_p^2 = 0.00$	$\chi^2 = 0.841$ $p = 0.359$ CI = 0.27 [−0.30, 0.84] $\omega_p^2 = 0.00$	

F: Anova F value, ω_p^2: Effect size (partial omega squared), Z: dividing the estimated coefficient by its standard error in ordinal logistic regression, t: t statistics value in Beta regression model, GLM: Generalised linear model, χ^2 = chi-squared value. CI (95 % confidence interval) represents the estimated effect sizes of high temperature, low pH, and their interaction on the response variable in the model. Significant effects are indicated by bold text.

Table 2
Paramuricea clavata statistical test results.

Parameter	Model	Temperature	pH	Temperature × pH	Time	Temperature × Time
Oxygen consumption	GLM gamma	**$\chi^2 = 4.805$** **$p = 0.029$** **CI = 0.64 [−0.27, 1.55]** **$\omega_p^2 = 0.08$**	$\chi^2 = 0.738$ $p = 0.390$ CI = −0.20 [−1.11, 0.71] $\omega_p^2 = 0.00$	$\chi^2 = 0.054$ $p = 0.815$ CI = −0.15 [−1.43, 1.12] $\omega_p^2 = 0.00$		
Polyp activity	Ordinal logistic regression	$Z = 1.290$ $p = 0.197$ CI = −0.51 [−1.04, 0.03]	$Z = 0.468$ $p = 0.639$ CI = 0.13 [−0.40, 0.66]		$Z = -0.938$ $p = 0.348$ CI = −0.14 [−0.44, 0.16]	**$Z = -2.114$** **$p = 0.034$** **CI = −0.49 [−0.04, −0.95]**
DNAm	Beta	**$t = -1.578$** **$p = 0.128$** **$\omega_p^2 = 0.07$**	**$t = -2.643$** **$p = 0.014$** **$\omega_p^2 = 0.08$**	$t = 2.568$ $p = 0.017$ $\omega_p^2 = 6.25 \times 10^{-3}$		
Carbohydrate	General linear	$F = 1.685$ $p = 0.206$ CI = −0.15 [−1.26, 0.97] $\omega_p^2 = 0.00$	$F = 0.000$ $p = 0.987$ CI = 0.34 [−0.77, 1.46] $\omega_p^2 = 0.00$	$F = 0.834$ $p = 0.370$ CI = −0.70 [−2.27, 0.88] $\omega_p^2 = 0.00$		
Protein	General linear	$F = 0.446$ $p = 0.510$ CI = −0.20 [−1.36, 0.96] $\omega_p^2 = 0.00$	$F = 0.023$ $p = 0.880$ CI = 0.13 [−1.03, 1.28] $\omega_p^2 = 0.00$	$F = 0.027$ $p = 0.870$ CI = −0.13 [−1.77, 1.51] $\omega_p^2 = 0.00$		
Lipid	GLM gamma	$\chi^2 = 3.130$ $p = 0.076$ CI = −0.30 [−0.73, 0.13] $\omega_p^2 = 0.06$	$\chi^2 = 0.622$ $p = 0.430$ CI = −0.15 [−0.58, 0.29] $\omega_p^2 = 0.00$	$\chi^2 = 0.019$ $p = 0.889$ CI = 0.04 [−0.58, 0.67] $\omega_p^2 = 0.00$		

F: Anova F value, ω_p^2: Effect size (partial omega squared), Z: dividing the estimated coefficient by its standard error in ordinal logistic regression, t: t statistics value in Beta regression model, GLM: Generalised linear model, χ^2 = chi-squared value. CI (95 % confidence interval) represents the estimated effect sizes of high temperature, low pH, and their interaction on the response variable in the model. Significant effects are indicated by bold text.

least one PFAM domain. Additionally, 45,041 genes (96.07 %) and 114,772 transcripts (86.93 %) were matched to at least one protein in the UniRef90 database. Analysis of all the assembled genes against both the KEGG orthology and GO databases, utilising the eggNOG mapper software, yielded 17,721 GO term matches and 20,113 KEGG Orthology (KO) entry matches (Fig. S3). Overall, the quality of the de novo assembled transcripts and their functional annotations support further downstream analysis.

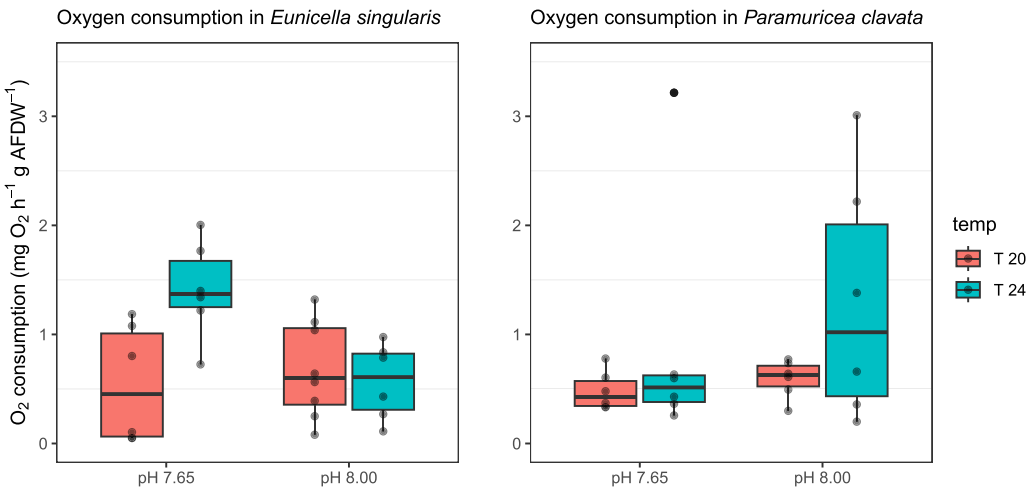

Fig. 3. Oxygen consumption (mg O_2 h^{-1} g $AFDW^{-1}$) in *E. singularis* and *P. clavata* exposed to four experimental conditions for two weeks: low temperature/low pH (20 °C, pH 7.65), low temperature/high pH (20 °C, pH 8.00), high temperature/low pH (24 °C, pH 7.65), and high temperature/high pH (24 °C, pH 8.00).

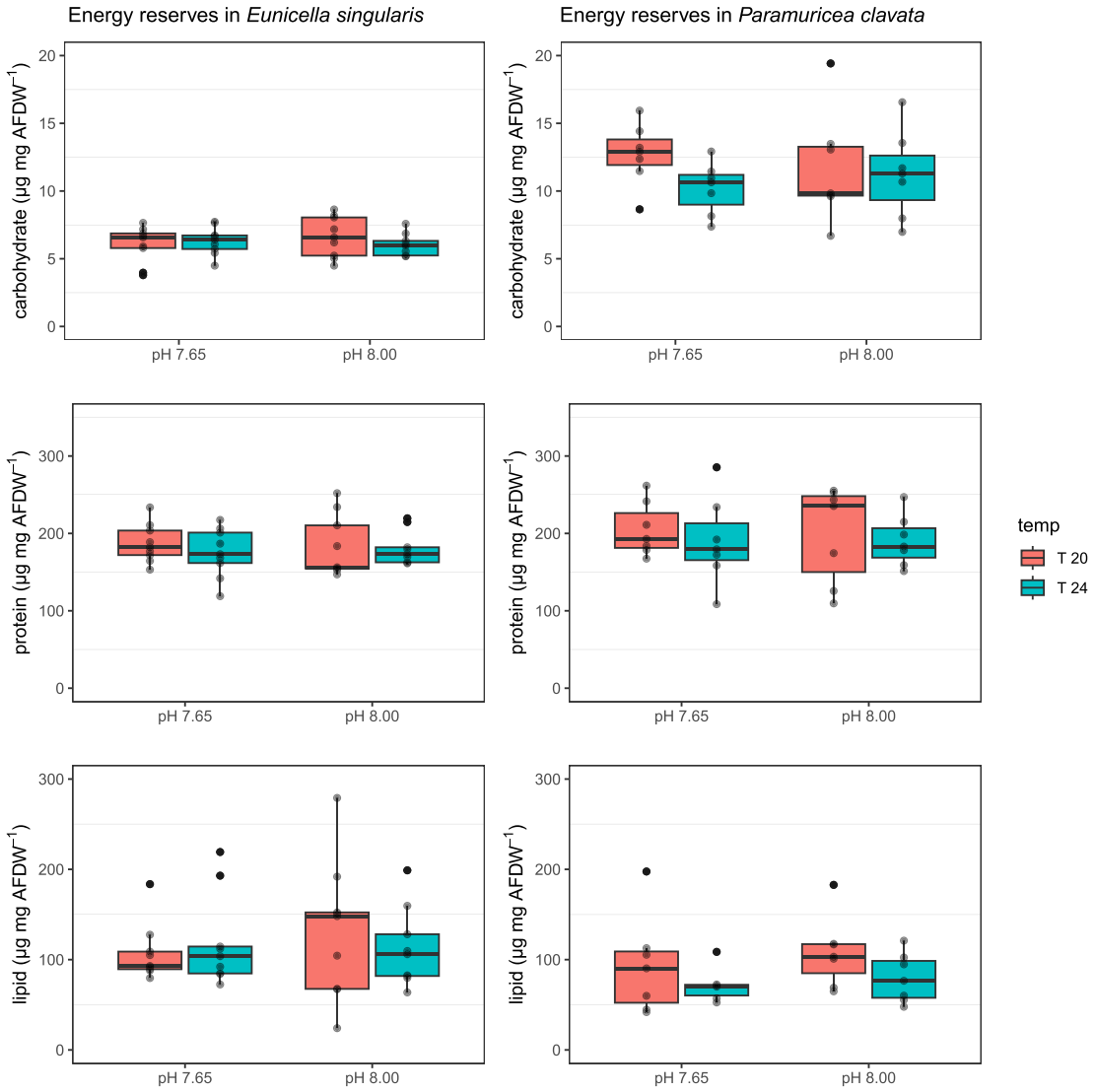

Fig. 4. Carbohydrate, protein and lipid contents (µg/mg AFDW) in *E. singularis* and *P. clavata* exposed to four experimental conditions for two weeks: low temperature/low pH (20 °C, pH 7.65), low temperature/high pH (20 °C, pH 8.00), high temperature/low pH (24 °C, pH 7.65), and high temperature/high pH (24 °C, pH 8.00).

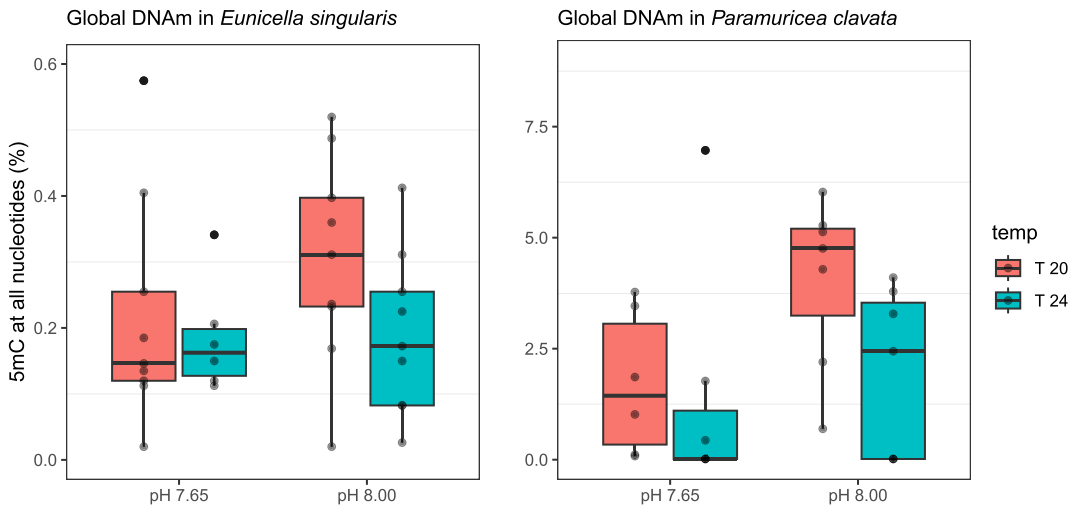

Fig. 5. Global DNA methylation (percentage of 5mC in all nucleotides) in *E. singularis* and *P. clavata* exposed to four experimental conditions for two weeks: low temperature/low pH (20 °C, pH 7.65), low temperature/high pH (20 °C, pH 8.00), high temperature/low pH (24 °C, pH 7.65), and high temperature/high pH (24 °C, pH 8.00).

3.4.2. Profiling gene expression in response to high temperature and low pH

We assessed global changes in gene expression patterns under high temperature/high pH, low temperature/low pH, high temperature/low pH conditions compared to low temperature/high pH condition to facilitate biological inferences at the transcriptome level. Thus, we were able to assess the response of the coral transcriptome to high temperature alone, low pH alone and their combination. Differentially expressed gene (DEG) analysis of the mRNA reads revealed that the combination of high temperature and low pH caused significant up- and downregulation of 121 and 443 unigenes, respectively. Notably, high temperature alone caused the greatest number of DEGs (6034 upregulated and 2360 downregulated unigenes). Low pH alone induced the lowest number of DEGs, 125 genes exhibited transcriptional changes, with 60 unigenes upregulated and 65 unigenes downregulated (Fig. S4, Dataset S1). However, at high temperatures, there were no statistically significant differences in the number of unigenes between low and high pH.

The heatmaps were also used to analyse the top 40 DEGs under high temperature/low pH, high temperature/high pH and low temperature/low pH compared with high pH/low temperature conditions (Fig. 7A–C). There were significant alterations in the expression of genes associated with various responses to the combination of high temperature and low pH. The analysis revealed that DEGs associated with diverse cellular processes were significantly upregulated under high-temperature/low-pH conditions, including apoptosis (e.g., A0A6S7FEL2, A0A7D9HMH2), cell cycle regulation (A0A7D9I1Q4, A0A6S7FL07), cell membrane structure and function (A0A6S7HPS5, UPI001F04D236), cell signalling (A0A6S7G9W3, A0A7D9DLC0), DNA repair/processing (A0AAD9Q0A2, UPI00106A4171), oxidative stress response (A0A6S7GVV0, UPI001068F957), and ubiquitination (A0A7D9DQV4, A0A6S7J4D9). High temperature alone elicited a similar pattern of upregulated DEGs, with notable overlap in functions related to apoptosis, cell cycle regulation, and oxidative stress response (Fig. 7A, B).

When the top 40 DEGs associated with the low pH alone condition were examined, the downregulated genes were involved in RNA processing (A0A6S7G2L3, A0A6S7GI61), protein modification (A0A6S7GE86, A0A7D9DCB6, A0A7D9DP44), metabolism (A0A7D9DQ04, UPI0010697389), cellular transport (UPI001069F167), signalling and regulation (UPI001069122F, UPI0010692ED2, UPI00106A7EF8), and gene expression (UPI001069E773, UPI00106A6F00, UPI00106B084F). The upregulated genes included genes involved in intracellular transport (A0A6S7FEL2), amino acid transport (A0A6S7FKN7), protein phosphorylation (A0A6S7FNL0, A0A6S7G9W3, UPI00106937C7), mRNA decapping (A0A6S7HJ70), DNA repair (A0A6S7I0B6), transcriptional regulation (A0A6S7K0I7), cell signalling (A0A6S7HPS5, UPI00106A33F5), and ubiquitination (UPI00106A8110). Additionally, some upregulated genes are involved in membrane transport (UPI0010696D68, UPI00106A2449), energy metabolism (UPI00106A0D6F), and cell cycle processes (UPI00106A4171) (Fig. 7C).

The enrichment analysis of GO biological processes revealed distinct cellular responses to high temperatures and low pH when corals were exposed to these factors either alone or in combination. The combination of high temperature and low pH markedly enriched biosynthetic and metabolic processes, such as translation, peptide biosynthesis, and nitrogen compound metabolism, indicating an increase in protein synthesis and metabolic activity to counteract the compounded stress (Fig. 7D). In contrast, high temperature alone enriched regulatory processes related to catabolism and protein dephosphorylation, with elevated fold enrichment values suggesting a strong emphasis on protein turnover and cellular quality control (Fig. 7E). Low pH alone also enhanced the regulation of catabolic processes and protein dephosphorylation, although to a lesser extent than high temperature did, indicating that pH stress primarily affects protein degradation pathways (Fig. 7F). Overall, these findings highlight that while high temperature alone predominantly triggers catabolic responses, the combination of high temperature and low pH activates both anabolic and catabolic pathways, suggesting broad and coordinated cellular adaptation (Fig. S5, Dataset S2). The RT-qPCR analysis was used to quantify the expression of selected genes (*HSP90*, *Str70*, *TNF5*, *TNF3*, *SOD*, *MB*, and *NEP1*) across the three experimental conditions, which were normalized to that of *Actin*. The results largely aligned with the RNA-Seq data, confirming the condition-specific modulation of *HSP90*, *Str70*, *NEP1*, and *SOD*, particularly under high temperature and the combination of high temperature and low pH. *TNF5* and *TNF3* were relatively stable, whereas MB was notably upregulated under high temperature alone condition (Fig. S6).

3.4.3. DEG-TFs and signalling pathways modulating coral resilience to warming and acidification

TFs have been extensively studied in vertebrates and model invertebrates, such as *Drosophila melanogaster*. Recent research has identified approximately 270,000 TFs across various species, categorised into 73 distinct families. As expected, TFs were much more highly detectable in the high temperature alone condition relative to other conditions. Notably, among the 73 TF families identified across animal

(A)

Number of Genes	54782
Number of Transcripts	144353
GC-content (%)	41.69
Total length (bp)	149028901
N50 sequence length (bp)	1554 (n = 26005)
Longest sequence (bp)	40071
Mean sequence length (bp)	1032
Shortest sequence (bp)	176
Median sequence length (bp)	642
N50 sequence length (bp)	1559
L50 sequence count	26821
Number of sequences > 1K (bp)	48451 (33.6% of total number)
Number of sequences > 10K (bp)	140 (0.1% of total number)
Number of core genes detected (BUSCO)	
Total number of core genes queried	954
Complete	870 (91.19%)
Complete + Partial	897 (94.03%)
Number of missing core genes	57 (5.97%)

(B)

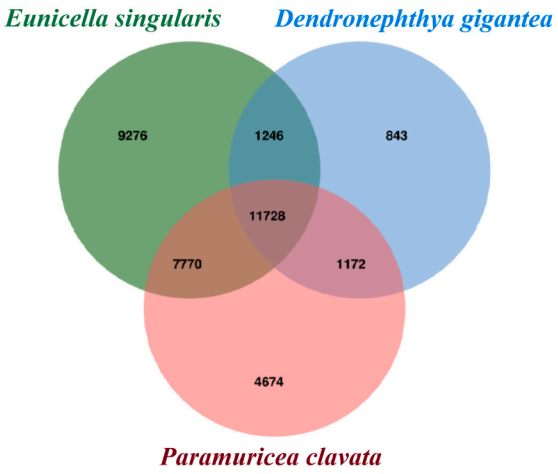

(C)

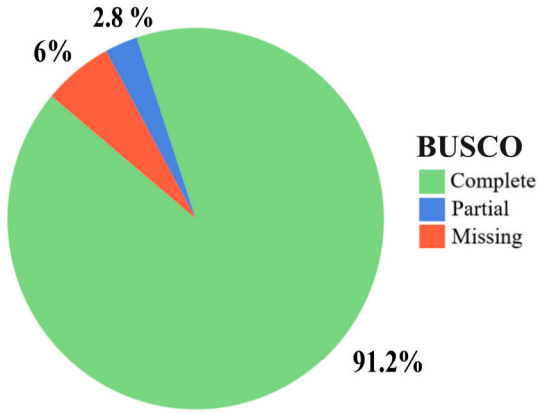

(D)

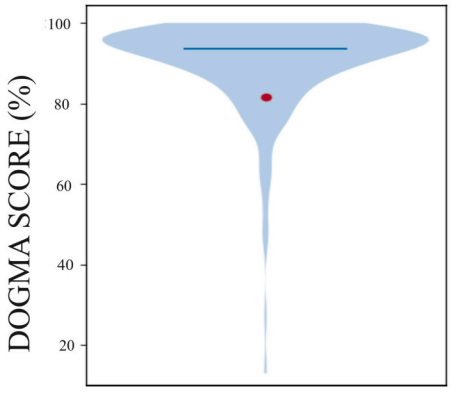

Fig. 6. (A) Summary statistics of the *de novo* transcriptome assembly of *E. singularis* generated by Trinity software. (B) Venn diagram showing the number of species-specific and overlapping coding sequence orthogroups among the three anthozoan transcriptome sequences. (C) Representation of BUSCO completeness assessment scores of *E. singularis* transcriptome dataset using metazoan-specific set of 954 single-copy core orthologs. (D) Completeness level of *E. singularis* transcriptome according to DOGMA analysis.

species, the *zf-C2H2*, *HMG*, *AP-2*, and *IRF* families were the most significantly represented among the differentially expressed TFs under high temperature/high pH condition (Fig. 8A). Intriguingly, most of the identified TFs were downregulated under these conditions. High temperature alone induced significant changes in the expression of various TFs, such as the downregulation of *AP-2*, *HMG*, and specific *zf-C2H2*. Specifically, downregulation was observed across *zf-C2H2* subtypes 1, 2, 3, 6, 7, 10, 11, 12, and 13 (Fig. 8B). Conversely, the transcription factors *IRF*, *RFX*, *P53*, and *NRF1* were upregulated, suggesting an increase in their activity or expression under high-temperature conditions (Fig. 8B, Dataset S3). These observations underscore the varied and contrasting impacts of high-temperature conditions on TFs expression, where certain TFs are suppressed, while others are activated. The identification of specific TFs and their corresponding expression patterns provides important insights into the molecular mechanisms that facilitate cellular adaptation to high temperature.

4. Discussion

4.1. Polyp activity, necrosis, and oxygen consumption

Alterations in oxygen consumption and polyp activity in gorgonians may disrupt their energy allocation, leading to reduced investment in reproduction. These physiological shifts can have cascading effects on individual fitness and the ecosystem services delivered by these organisms. While polyp contraction lowers feeding efficiency and respiration, polyp expansion increases oxygen diffusion and consumption in the tissue (Previati et al., 2010). In the present study, both polyp activity and the OCR increased in *E. singularis* at high temperatures, whereas the OCR but not polyp activity increased in *P. clavata* at high temperatures. The polyp activity measurement and the oxygen consumption test were not conducted simultaneously, which may obscures their possible correlation.

Previati et al. (2010) reported a decrease in polyp activity in *E. singularis* and *P. clavata* at high temperatures >18 °C. The difference between the two studies could be explained by the distinct natural temperature variability at the locations where the corals were collected.

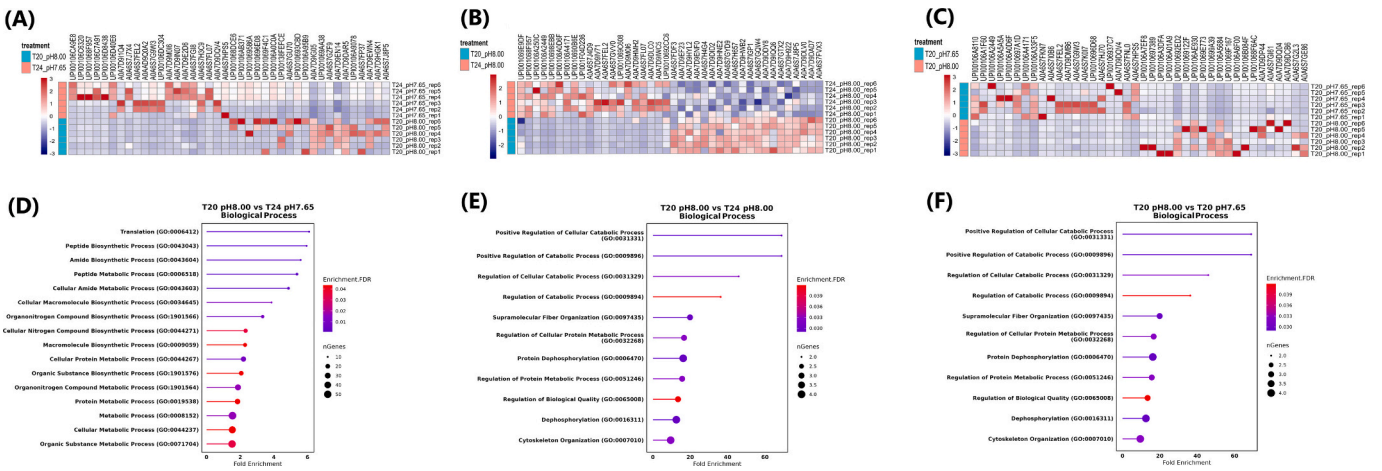

Fig. 7. Heatmaps illustrating the top 40 DEGs expression across different treatment comparisons, along with enriched GO biological process terms. Panels (A), (B), and (C) compare gene expression under different temperature and pH conditions: (A) 20°C, pH 8.00 vs. 24°C, pH 7.65, (B) 20°C, pH 8.00 vs. 24°C, pH 8.00, and (C) 20°C, pH 8.00 vs. 20°C, pH 7.65. The heatmaps were constructed using Rlog-normalized count data, where colour intensity reflects expression levels (blue for lower expression, red for higher expression). Panels (D), (E), and (F) display lollipop plots representing enriched GO biological processes associated with DEGs for each comparison. The dot sizes in the plots indicate the number of associated DEGs, the line length represents fold enrichment, and the dot colour denotes FDR, highlighting significant processes with FDR <0.05. Specifically, panel (D) shows GO enrichment for the comparison between 20°C, pH 8.00 vs. 24°C, pH 7.65, panel (E) compares 20°C, pH 8.00 vs. 24°C, pH 8.00, and panel (F) compares 20°C, pH 8.00 vs. 20°C, pH 7.65.

In the same study, complete polyp retraction at 25 °C, necrosis and mortality above 25 °C were reported in *P. clavata*, which was not the case in the current study at 24 °C for two weeks, even when high temperature was combined with low pH. Previati et al. (2010) reported that among the four octocoral species (*Eunicella cavolini*, *E. singularis*, *Corallium rubrum*, *P. clavata*) *P. clavata* is the most sensitive, whereas *E. singularis* is the most resistant to high temperatures.

In the present study, high temperature and low pH did not cause necrosis or tissue death in the gorgonians. Consistent with our results, four gorgonian species, including *P. clavata*, presented no death after 134 days of high-temperature exposure (24 °C and above) (Pereira, 2019). Pey et al. (2011) reported polyp retraction in *E. singularis* at 26 °C but no necrosis or mortality at 19 days of exposure. In another study, Pey et al. (2013) reported tissue necrosis and thinning at 26 °C and severe tissue necrosis in *E. singularis* above 26 °C under laboratory conditions, regardless of the depth and location where corals were collected (along the coasts of France and Spain). Together, variable thermotolerance has been reported in different regions of the Mediterranean Sea for the two species studied. The high temperatures tested in the present study fall within the upper thermal limits of those two species, which are in the range of 23–26 °C according to several studies. Vargas et al. (2017, 2022) demonstrated that experimental scenarios should be considered in the context of the present range of variability and that physiological thresholds tend to be correlated with the extremes of this range. The selected temperature levels in the current study slightly deviate from the present range of variability at the collection site and might cause a true stress response in corals.

In the NW Mediterranean, <5 %, >15 % and >85 % necrosis were recorded in *E. singularis* during the 2003 marine heat wave at 25.5, 26.5 and 28.5 °C, respectively (Garrabou et al., 2009). Crisci et al. (2017) used various distant populations of *P. clavata* in a common garden experiment. They reported that the critical thermal threshold was 25 °C. Gómez-Gras et al. (2022) performed a similar study on far populations of *P. clavata* and reported that 25 °C is lethal if exposure is extended, resulting in complete mortality at 25 days. Our study, in which the selected high temperature was 24 °C, confirmed that <25 °C is not lethal for *P. clavata* for two weeks, even if it is combined with low pH. Longer exposure to 24 °C and above has been shown to negatively affect gorgonian health (Tignat-Perrier et al., 2022; Lange et al., 2023). Local adaptation and/or acclimation to warmer conditions have a limited effect on the response of *P. clavata* to thermal stress (Crisci et al., 2017; Gómez-Gras et al., 2022). Gorgonians that are adapted to high fluctuations in temperature and pH in their natural environment are possibly resistant to tested scenarios owing to their preadapted physiological capacities (acclimation) and phenotypic plasticity.

Holobiont performance can be estimated by respiration rates because it is dominated by whole-organism physiology rather than symbionts, whereas photosynthesis is driven by symbionts (Jurriaans et al., 2021). In the present study, the OCRs of *E. singularis* and *P. clavata* were significantly greater at 24 °C than at 20 °C. Similarly, Jurriaans et al. (2021) reported an elevated OCR at 20 and 23 °C compared with the ambient temperature of 18 °C and calculated the thermal breadth as 23.5 ± 1.9 °C. Lange et al. (2023) reported that the respiration rate increased in both species at 24 °C compared with that at 17 °C. In contrast, Previati et al. (2010) reported that less oxygen was consumed at 25 °C than at 18–20 °C. In the current study, the physiology of *E. singularis* might be fine-tuned with the help of increased polyp activity when exposed to a combination of high temperature and low pH, as well as increased OCR when exposed to high temperature alone. The same response was also observed in *P. clavata* for the OCR. Increased metabolism is thought to be a response to increased energy demands resulting from elevated temperatures and decreased pH levels (Sokolova, 2021). Marine animals can increase their oxygen consumption to compensate for the excessive energy budget (Pörtner et al., 2004). Increased metabolic rates have been shown in response to elevated temperatures across the thermal tolerance window of corals (Pörtner, 2008). The increased metabolic activity associated with high temperatures could also provide excess energy for the acid-base regulation during seawater acidification (Khalil et al., 2023). There might be a regulatory trade-off between metabolic physiology and other physiological functions (Khalil et al., 2023) in corals to cope with high temperature and low pH. Overall, the variability in response results obtained in terms of polyp activity, necrosis and oxygen consumption in the above studies can be explained by (i) the intensity of the tested scenario (ii) the species-specific regulatory trade-off between physiological functions and metabolic physiology, and (iii) the natural variability of temperature and pH in the collection sites.

4.2. Energy reserves

An organism's energy demand and the environment's energy supply become more out of balance as the pH challenge level increases. This

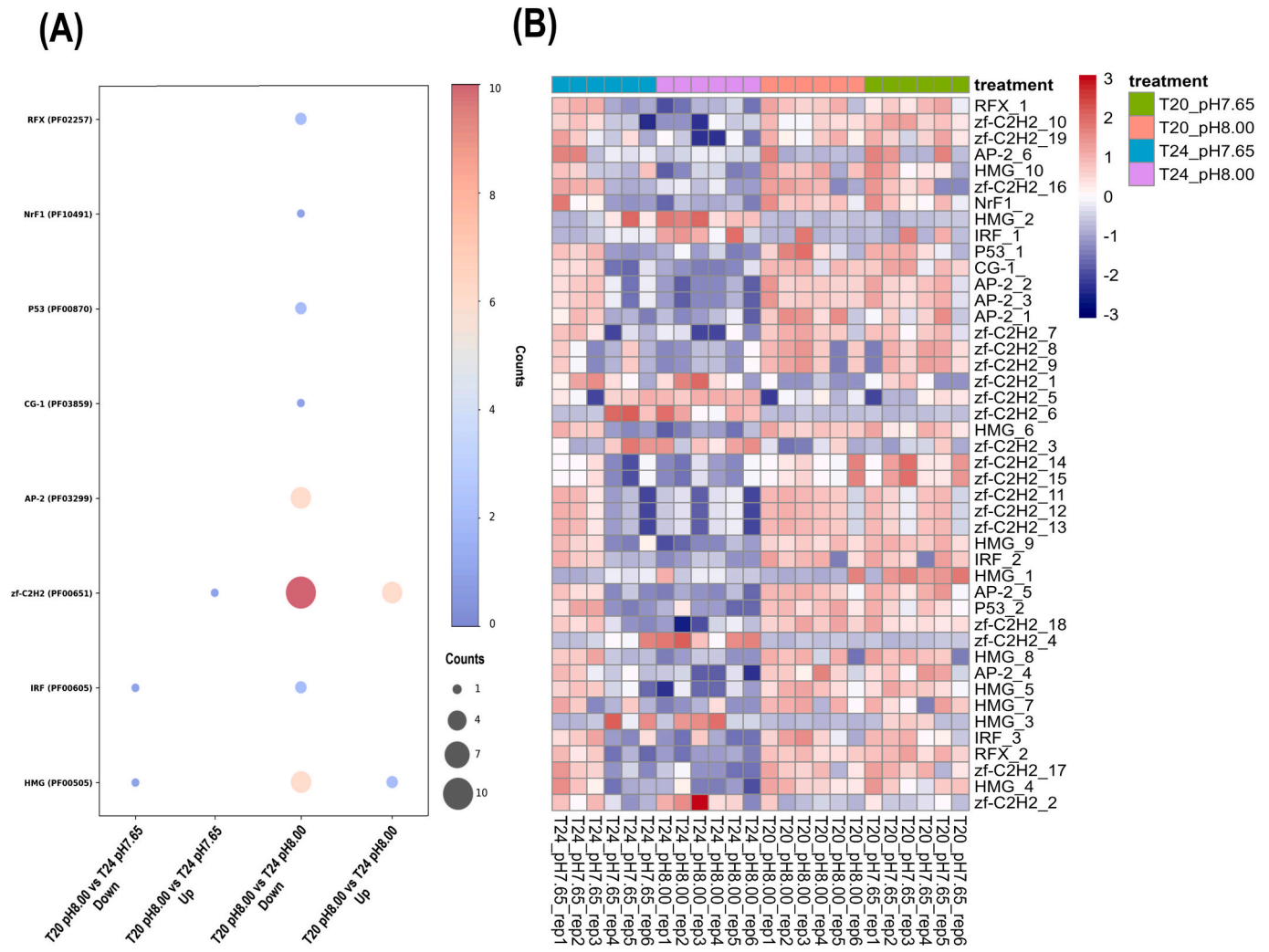

Fig. 8. The panel illustrates DEGs encoding TFs and their expression profiles across various treatments. (A) The dot plot depicts the number of DEGs associated with different TF families across treatment groups, highlighting up and downregulated DEGs. (B) The heatmap displays the expression patterns of these TFs across the treatments, with a colour scale transitioning from blue (indicating low expression) to red (indicating high expression).

leads to the depletion of tissue energy reserves such as glycogen, lipids, and proteins and ultimately has a detrimental effect on survival and fitness (Sokolova, 2021). Tignat-Perrier et al. (2022) reported decreased carbohydrate, lipid, lactate and stable protein concentrations in *P. clavata* exposed to thermal stress (16 vs. 24 °C) during seven weeks. Pey et al. (2011) studied the total oxyradical scavenging capacity (TOSC), ubiquitinated protein and heat-shock protein (HSP70) levels in *E. singularis* to assess cellular stress and stated that 24 °C did not cause stress, whereas 26 °C did. Lange et al. (2023) demonstrated decreased lipids in *P. clavata* when they were exposed to 24 °C for two weeks compared with 17 °C, whereas lipids are stable in *E. singularis*. In the current study, energy reserves were not affected by temperature, pH or their interaction. Proteins serve as the body's last energy reserve, which is employed in times of acute energy shortage (e.g., hunger) or brief periods of intense energy demand (Falfushynska et al., 2019; Haider et al., 2018). Corals can catabolize their lipid reserves to compensate for energy consumption derived from thermal and pH regulation (McCauley et al., 2018; Rodrigues and Grottoli, 2007). In a previous study, a reduced lipid content was shown in *E. singularis* when it was exposed to thermal stress (24 vs. 26 °C) for one and three weeks (Ezzat et al., 2013). The inconsistent results of the present study, i.e., the constant energy reserves in gorgonians under high-temperature conditions, can be explained as follows: (i) symbionts could aid in keeping the energy reserves in the symbiotic species *E. singularis*, (ii) the incubation time could be shorter than the time needed to observe biochemical changes in both the symbiotic species *E. singularis* and the aposymbiotic species *P. clavata*, and (iii) there can be a trade-off between energy reserves and other physiological functions.

4.3. Global DNA methylation and transcriptome profile

DNAm, an important indicator of changes in the epigenome profile, is crucial for rapid acclimation to environmental changes in long-living corals. Earlier studies have shown that epigenetic mechanisms such as DNAm in scleractinian corals could offer them a greater ability to buffer the impacts of warming and acidification by fine-tuning gene expression (Putnam et al., 2016; Putnam, 2021; Liew et al., 2018; Dimond and Roberts, 2016; Aranda Lastra, 2022). While the results of the current study did not allow us to discuss gene regions and gene-specific methylation patterns, we could present gDNAm in gorgonian species. The estimates of gDNAm rates typically do not identify "seesaw" patterns with comparable increases and decreases in DNAm in various regions of the genome. This may lead to a neutralising impact that generates essentially identical gDNAm rates between treatments (Ishida-Castañeda et al., 2023). In support of this view, Guerrero and Bay (2024) demonstrated a strong association between differential expression and DNAm in 461 gene bodies, despite the lack of relationship between gDNAm and transcriptional plasticity.

In the present study, the presence of gDNAm was confirmed for the first time in gorgonian octocorals, *E. singularis* and *P. clavata*. The gDNAm level in *E. singularis* is similar to that in other invertebrates (especially corals) (Putnam et al., 2016; Liew et al., 2018) but is expectedly much lower than that in mammals (Beal et al., 2020). In a previous study, gDNAm was detected in 72 of 76 octocoral species (123 samples) (Walling, 2020). Walling (2020) reported substantial interspecific and intraspecific variation in gDNAm in octocorals, and the average gDNAm was 1.16 %, ranging from 0 to 6.93 %. The only octocoral gorgon species for which gDNAm was reported was *Leptogorgia virgulata*, which has a relatively high gDNAm of 2–6 % (Walling, 2020). gDNAm in *P. clavata* was relatively greater than that in *E. singularis* (this study), 76 octocoral species (Walling, 2020) and scleractinian corals (Putnam et al., 2016; Liew et al., 2018; Dimond and Roberts, 2016). CpG islands are regions of DNA that have a high frequency of CG (cytosine guanine) dinucleotides. In invertebrates, including corals, DNA methylation occurs primarily on CpG islands within gene bodies (Dixon et al., 2016; Liew et al., 2018). Seven percent and 8 % of the CpG islands have been reported to be methylated in the corals *Stylophora pistillata* (Liew et al., 2018) and *Acropora nana* (Guerrero and Bay, 2024), respectively. Since we determined the degree of methylation of all the nucleotides, it was not possible to directly compare the degree of methylation with that reported in those studies. However, methylation in CpG islands must be greater in *P. clavata* than in other species since even gDNAm is approximately 2.2 %. However, considering that the number of bases and genes in the *P. clavata* genome is much greater than that in other species (Macleod et al., 2023), the high gDNAm (2.2 %) detected in our study is thought to be correlated with methylation in CpG islands. In addition to CpG islands, DNA methylation also occurs at repetitive sequences. These sequences are involved in a variety of cellular processes. Since they can cause genome instability, most repetitive elements are usually methylated to maintain a heterochromatic repressed state. Hypomethylation of repetitive sequences is associated with chromatin relaxation and irregular transcription (Pappalardo and Barra, 2021). Although the proportion of repeat sequences in the *E. singularis* genome is unknown, it has recently been determined that the *E. verrucosa* genome contains 46 % repeat sequences (Macleod et al., 2023). The *P. clavata* genome contains 49 % repeat sequences (Ledoux et al., 2020). The approximately 10-fold greater gDNAm in *P. clavata* than in *E. singularis* may be due to a difference in the methylation of the repeat sequences. From this point of view, *P. clavata* can be considered to have a more protected heterochromatic structure under normal conditions. In the present study, high temperature significantly suppressed gDNAm in *P. clavata*. This finding suggests that the heterochromatic genome, which is normally protected by methylation, may have transformed into a loose euchromatic structure due to the loss of methylation caused by the effect of increasing temperature. This change can significantly affect gene expression and genomic stability.

In the current study, we observed a species-specific pattern as a response to warming and acidification. DNAm is a dynamic process, and varies by taxon, species life stage and the intensity and duration of environmental change. A significant increase in gDNAm was shown in the reef-building coral *Stylophora pistillata* (Liew et al., 2018) at pH: 7.2 and in the scleractinian coral *Pocillopora damicornis* at pH: 7.35–7.60 (Putnam et al., 2016). Constant gDNAm has been shown in the ascidian *Didemnum vexillum*, which was exposed to variable salinity (Hawes et al., 2018), and the stony coral *Pocillopora damicornis*, which was exposed to thermal stress (Jiang et al., 2024). Contrasting responses of symbiotic conditions of primary polyps of the coral *Acropora digitifera*, such as decreased gDNAm in aposymbiosis and increased gDNAm in symbiont, to thermal stress have been demonstrated (Ishida-Castañeda et al., 2023). Additionally, life-stage-dependent methylation has been shown, such as more pronounced methylation in larvae than in adults in the coral *Pocillopora damicornis* (Jiang et al., 2024) and in the marine fish *Dicentrarchus labrax* (Anastasiadi et al., 2017). Global and CpG DNAm are not altered by heat stress in the reef-building coral *Acropora nana* (Guerrero and Bay, 2024). Like the current study, most of the above-mentioned studies did not consider gene region-specific DNAm, which could have obscured the causative relationship between the DNAm and environmental stress tested in these studies.

Transcriptional plasticity is crucial for facilitating adaptive phenotypic plasticity in corals under unfavourable conditions, such as thermal and acidification stress (Guerrero and Bay, 2024). During environmental changes, transcriptional plasticity may lead to a broad range of plasticity in physiology, morphology, or behaviour over the lifetime of an individual and shape species fitness. According to earlier research, the degree of the transcriptional response to acute heat stress can be influenced by temperature adaptation acquired via (trans)generational memory (Bay and Palumbi, 2015; Hackerott et al., 2021).

In the current study, high temperature alone resulted in many more DEGs (8400), than did the combination of high temperature and low pH (560) or low pH alone (125) in the *E. singularis* holobiont. This finding indicates that high temperature alone is the primary driver of the transcriptomic plasticity in *E. singularis*. In contrast, the coral hosts *Acropora valida* and *Galaxea fascicularis* subjected to the combination of warming and acidification presented greater numbers of DEGs than those exposed to either warming or acidification alone (Wu et al., 2023). These authors reported that low pH alone caused the fewest DEGs, which is in line with our findings. The same pattern (DEGs: acidification × warming > warming > acidification) was also reported in the larvae of coral *Pocillopora damicornis* (Jiang et al., 2022). Consistent with the result of the present study, Davies et al. (2016) reported greater DEGs in *Siderastrea siderea* coral exposed to higher temperature (28 vs. 32 °C) than in those exposed to high pCO_2 (477 vs. 600 and 2550 μatm). The gene expression profile differences between this study and other studies (e.g., interactive effects) may be due to the degree of deviation between the natural temperature and pH variations where the corals were collected and the levels applied in the laboratory. This idea is supported by the fact that the aforementioned studies reported observable effects (bleaching, etc.), contrary to this study. These results also show that the effects of the two stressors combined cannot be inferred from the effects of the single stressors to which the corals were exposed. This is not surprising because our experimental design is unable to resolve the nonlinear dose-response relationship across a temperature and pH range (Boyd et al., 2018). To completely comprehend the combined impacts, an additional experimental design, such as resolving performance curves for each driver and possible interactions, is needed.

TFs play a pivotal role in orchestrating the complex gene expression changes necessary for corals to adapt to environmental stress, including high temperatures. The response of coral transcripts to high-temperature stress reveals a complex molecular landscape of cellular adaptation (Avila-Magaña et al., 2021; Savary et al., 2021; Jia et al., 2024). A comprehensive literature review reveals limited research on the relationship between TF and coral adaptation to stressors. Our findings demonstrate significant differential expression across several TF families, highlighting the intricate regulatory mechanisms triggered primarily by high temperature. The downregulation of *zf-C2H2*, *HMG*, and *AP-2* families, alongside the upregulation of *IRF*, *P53*, and *NRF1*, suggests a complex interplay of molecular mechanisms regulating stress responses and maintaining cellular homeostasis under high-temperature stress conditions. The *zf-C2H2* (Zinc Finger C2H2) TFs are involved in various functions, including development, cellular differentiation, and stress response in animals (Sebé-Pedrós and de Mendoza, 2015; Mukherjee and Moroz, 2024). Downregulation of several *zf-C2H2* subtypes may indicate suppressed nonessential gene expression and a shift in cellular priorities toward survival pathways. Downregulation of HMG (high mobility group) proteins under thermal stress could signify reduced chromatin remodelling activity, potentially limiting transcriptional flexibility to conserve energy. A recent study discovered an HMG protein called DSP1 that directly interacts with and negatively regulates the HSP70 promoter in the oyster *Crassostrea hongkongensis*, playing a critical role in heat shock response by modulating the transcription of

HSPs and thereby helping to regulate cellular stress mechanisms (Miao et al., 2016). The downregulation of the *AP-2* gene suggests a potential impairment in the coral's genetic stress response mechanism during thermal challenges. Tom et al. (1999) suggested that various TF motifs, including the *AP-2* motif, may be involved in the regulation of *SP-HSP70* transcription in response to stress in the coral *Stylophora pistillata*.

The upregulation of *IRF*, *P53*, and *NRF1* (Nuclear Respiratory Factor 1) TFs indicates an active cellular defence mechanism in corals (Hemond and Vollmer, 2015). Interferon Regulatory Factors (*IRFs*) are not directly associated with heat stress, but they are central to immune responses and stress adaptation, regulating apoptosis and cellular repair mechanisms (Negishi et al., 2018). Their upregulation suggests an enhanced immune-like response and cellular protection under high-temperature conditions (Haslun et al., 2018).We also observed the upregulation of *NRF1*, which is primarily recognised as a transcription factor regulating oxidative stress responses, mitochondrial biogenesis, oxidative phosphorylation, and cellular energy metabolism in many organisms, including corals (Bennett et al., 2022). Its increased expression suggests an active role in mitigating reactive oxygen species (ROS) accumulation, a common consequence of thermal stress in metazoans (Doonan et al., 2019). Our findings align with previous research demonstrating the upregulation of the *p53* gene. Its upregulation indicates a protective role, likely facilitating the repair of thermal stress-induced DNA damage and promoting cell survival (Helton and Chen, 2007). For instance, studies on *Orbicella faveolata* have shown that p53 proteins are overexpressed following heat stress, which is associated with DNA damage and coral bleaching (Lesser and Farrell, 2004). Additionally, another study found that genes associated with the p53 signalling pathway were enriched in *Pocillopora damicornis* corals exposed to temperatures of 31 °C and 32 °C, contributing to the expulsion of algal symbionts (Li et al., 2021).

TF findings collectively indicate a reprogramming of the coral transcriptome under thermal stress. The suppression of TFs associated with development and chromatin remodelling, alongside the activation of stress-responsive and repair-associated TFs, reflects an adaptive strategy to manage the dual challenges of proteotoxic stress and oxidative damage. These transcriptional shifts could help corals maintain cellular integrity and improve survival under high-temperature conditions. Future studies investigating the direct target genes of these TFs will enhance our understanding of the molecular pathways driving thermal stress resilience in corals.

Transcriptional and epigenomic plasticity have also been studied jointly under environmental changes. A positive correlation between gene body DNAm and transcription was reported in the scleractinian coral *Stylophora pistillata* (Liew et al., 2018). Gavery and Roberts (2013) also reported a positive correlation between DNAm and transcription in oysters. However, very recent studies have demonstrated that there is no correlation between gene expression and DNAm in corals, both at the gene and global levels (Abbott et al., 2024; Guerrero and Bay, 2024; Dixon and Matz, 2022). The findings of the current study did not allow us to discuss the relationship between the gene/gene region-specific transcriptome and DNAm. However, temperature did not affect the gDNAm of *E. singularis*, although temperature alone induced a very high number of DEGs in the transcriptome. The seesaw pattern might have masked the alteration in gDNAm in *E. singularis* (Ishida-Castañeda et al., 2023). Compared with *E. singularis*, *P. clavata* is more vulnerable to environmental changes such as warming (Previati et al., 2010; Ezzat et al., 2013; Capdevila et al., 2024). In that context, gDNAm in the sensitive coral *P. clavata* was affected by either warming or the combination of warming and acidification, whereas gDNAm in the resistant coral *E. singularis* was not affected by warming or acidification. Similarly, Putnam et al. (2016) reported that acidification affected gDNAm in the sensitive coral *Pocillopora damicornis* but not in the resistant coral *Montipora capitata*. Observed transcriptomic and DNA methylation changes in the current study are not concluded as adaptive phenotypic plasticity due to: 1) they do not provide information about transgenerational heritability, 2) the fate of these traits in a long-term or repeated exposure is not known. However, phenotypic plasticity shown in the current study can be stabilised by genetic or epigenetic mechanisms over time and has the potential to improve corals' fitness.

The combined effect of high temperature and low pH could not be predicted by a simple arithmetic additive response at the effect level, highlighting more complex and nonlinear effects. For example, the combined effects of high temperature and low pH on DEGs seem antagonistic rather than additive in *E. singularis*. Future work should address the gene-specific DNAm profile, transcriptome and physiology by using a gradient of temperature/pH rather than a scenario-based approach to better understand the relative contribution of each driver to the overall stress response. Also, as shown in the current study, warming is the primary driver of change in the gorgonian species living in Aegean Sea. Conservation studies should be implemented in the region to improve the resilience of these species to marine heat waves, leading to seawater temperatures of 24 °C and above during several weeks.

5. Conclusion

Warming, acidification and their combination did not cause necrosis or mortality in both species. Oxygen consumption increased in both species at high temperatures. Energy reserves were not affected by temperature, pH or their interaction in either species. Global DNAm rate was ten times higher in *P. clavata* than in *E. singularis*. gDNAm in *P. clavata* decreased at high temperatures and when high temperature and low pH were combined. High temperature alone caused significantly more DEGs than low pH alone, and the combination of high temperature and low pH in *E. singularis*. Overall warming and the combination of warming and acidification induced physiological, transcriptomic and epigenetic alterations in both species. These changes shape the fitness of these species and negatively impact associated ecosystems.

Supplementary data to this article can be found online at https://doi.org/10.1016/j.scitotenv.2025.179845.

CRediT authorship contribution statement

Murat Belivermiş: Writing – review & editing, Writing – original draft, Visualization, Methodology, Investigation, Funding acquisition, Formal analysis, Conceptualization. **Önder Kılıç:** Investigation, Funding acquisition, Conceptualization. **H. Barış Özalp:** Writing – original draft, Resources, Investigation. **Selcan Demiralp:** Resources, Methodology, Investigation. **Selda Gezginci-Oktayoglu:** Validation, Methodology, Investigation. **Vahap Eldem:** Writing – original draft, Investigation, Formal analysis. **Berna Şahin:** Resources, Investigation. **Mehmet Ali Balcı:** Methodology. **Selahattin Barış Çay:** Methodology. **Onur Gönülal:** Resources.

Declaration of competing interest

The authors declare that they have no known competing financial interests or personal relationships that could have appeared to influence the work reported in this paper.

Acknowledgements

This study was funded by Scientific Research Projects Coordination Unit of Istanbul University. Project number: 38485. We thank Narin Sezer for their excellent technical assistant.

Data availability

Data will be made available on request.

References

Abbott, E., Loockerman, C., Matz, M.V., 2024. Modifications to gene body methylation do not alter gene expression plasticity in a reef-building coral. Evolutionary Applications 17 (2), e13662. https://doi.org/10.1111/eva.13662.

Anastasiadi, D., Díaz, N., Piferrer, F., 2017. Small ocean temperature increases elicit stage-dependent changes in DNA methylation and gene expression in a fish, the European sea bass. Sci. Rep. 7 (1), 12401. https://doi.org/10.1038/s41598-017-10861-6.

Aranda Lastra, M., 2022. Epigenetics and acquired tolerance to environmental stress. In: Coral Reef Conservation and Restoration in the Omics Age, pp. 135–150. https://doi.org/10.1007/978-3-031-07055-6_9.

Avila-Magaña, V., Kamel, B., DeSalvo, M., Gómez-Campo, K., Enríquez, S., Kitano, H., Medina, M., 2021. Elucidating gene expression adaptation of phylogenetically divergent coral holobionts under heat stress. Nat. Commun. 12 (1), 5731. https://doi.org/10.1038/s41467-021-25950-4.

Barton, A., Hales, B., Waldbusser, G.G., Langdon, C., Feely, R.A., 2012. The Pacific oyster, *Crassostrea gigas*, shows negative correlation to naturally elevated carbon dioxide levels: implications for near-term ocean acidification effects. Limnol. Oceanogr. 57 (3), 698–710. https://doi.org/10.4319/lo.2012.57.3.0698.

Bay, R.A., Palumbi, S.R., 2015. Rapid acclimation ability mediated by transcriptome changes in reef-building corals. Genome Biol. Evol. 7 (6), 1602–1612. https://doi.org/10.1093/gbe/evv085.

Beal, A., Rodriguez-Casariego, J., Rivera-Casas, C., Suarez-Ulloa, V., Eirin-Lopez, J.M., 2020. Environmental epigenomics and its applications in marine organisms. In: Population Genomics: Marine Organisms, pp. 325–359. https://doi.org/10.1007/13836_2018_28.

Belivermiş, M., Besson, M., Swarzenski, P., Oberhaensli, F., Taylor, A., Metian, M., 2020. Influence of pH on Pb accumulation in the blue mussel, *Mytilus edulis*. Mar. Pollut. Bull. 156, 111203. https://doi.org/10.1016/j.marpolbul.2020.111203.

Belivermiş, M., Kılıç, Ö., Gezginci-Oktayoglu, S., Sezer, N., Demiralp, S., Şahin, B., Dupont, S., 2023. Physiological and gene expression responses of the mussel *Mytilus galloprovincialis* to low pH and low dissolved oxygen. Mar. Pollut. Bull. 187, 114602. https://doi.org/10.1016/j.marpolbul.2023.114602.

Bennett, C.F., Latorre-Muro, P., Puigserver, P., 2022. Mechanisms of mitochondrial respiratory adaptation. Nat. Rev. Mol. Cell Biol. 23 (12), 817–835. https://doi.org/10.1038/s41580-022-00506-6.

Boyd, P., Collins, S., Dupont, S., Fabricius, K., Gattuso, J.P., Havenhand, J., Hutchins, D., Riebesell, U., Rintoul, M., Vichi, M., Biswas, H., Gao, K., Gehlen, M., Hurd, C., Kurihara, H., McGraw, C., Navarro, J., Nilsson, G., Passow, U., Pörtner, H.O., 2018. Experimental strategies to assess the biological ramifications of multiple drivers of ocean global changes – a review. Glob. Chang. Biol. 24, 2239–2261. https://doi.org/10.1111/gcb.14102.

Bramanti, L., Movilla, J., Guron, M., Calvo, E., Gori, A., Dominguez-Carrió, C., Grinyó, J., Lopez-Sanz, A., Martinez-Quintana, A., Pelejero, C., Ziveri, P., Rossi, S., 2013. Detrimental effects of ocean acidification on the economically important Mediterranean red coral (*Corallium rubrum*). Glob. Chang. Biol. 19 (6), 1897–1908. https://doi.org/10.1111/gcb.12171.

Bryant, D.M., Johnson, K., DiTommaso, T., Tickle, T., Couger, M.B., Payzin-Dogru, D., Lee, T.J., Leigh, N.D., Kuo, T.H., Davis, F.G., Bateman, J., Bryant, S., Guzikowski, A. R., Tsai, S.L., Coyne, S., Ye, W.W., Freeman Jr., R.M., Peshkin, L., Tabin, C.J., Regev, A., Haas, B.J., Whited, J.L., 2017. A tissue-mapped axolotl de novo transcriptome enables identification of limb regeneration factors. Cell Rep. 18, 762–776. https://doi.org/10.1016/j.celrep.2016.12.063.

Bucchini, F., Del Cortona, A., Kreft, L., Botzki, A., Van Bel, M., Vandepoele, K., 2021. TRAPID 2.0: a web application for taxonomic and functional analysis of de novo transcriptomes. Nucleic Acids Res. 49. https://doi.org/10.1093/nar/gkab565.

Cai, W.J., Hu, X., Huang, W.J., Murrell, M.C., Lehrter, J.C., Lohrenz, S.E., Chou, Y., Zhai, W.C., Gong, G.C., 2011. Acidification of subsurface coastal waters enhanced by eutrophication. Nat. Geosci. 4 (11), 766–770. https://doi.org/10.1038/ngeo1297.

Cantalapiedra, C.P., Hernandez-Plaza, A., Letunic, I., Bork, P., Huerta-Cepas, J., 2021. eggNOG-mapper v2: functional annotation, orthology assignments, and domain prediction at the metagenomic scale. Mol. Biol. Evol. 38, 5825–5829. https://doi.org/10.1093/molbev/msab293.

Capdevila, P., Zentner, Y., Rovira, G.L., Garrabou, J., Medrano, A., Linares, C., 2024. Mediterranean octocoral populations exposed to marine heatwaves are less resilient to disturbances. J. Anim. Ecol. https://doi.org/10.1111/1365-2656.14147.

Cole, V.J., Parker, L.M., O'Connor, S.J., O'Connor, W.A., Scanes, E., Byrne, M., Ross, P. M., 2016. Effects of multiple climate change stressors: ocean acidification interacts with warming, hyposalinity, and low food supply on the larvae of the brooding flat oyster *Ostrea angasi*. Mar. Biol. 163, 1–17. https://doi.org/10.1007/s00227-016-2880-4.

Cornwall, C.E., Comeau, S., Kornder, N.A., Perry, C.T., van Hooidonk, R., Lowe, R.J., 2021. Global declines in coral reef calcium carbonate production under ocean acidification and warming. Proceeding of the National Academy of Sciences, USA 118, e2015265118. https://doi.org/10.1073/pnas.2015265118.

Cornwall, C., Comeau, S., Harvey, B., 2023. Physiological and ecological tipping points caused by ocean acidification. Earth System Dynamics Discussions 2023, 1–21. https://doi.org/10.5194/esd-15-671-2024.

Crisci, C., Ledoux, J.B., Mokhtar-Jamaï, K., Bally, M., Bensoussan, N., Aurelle, D., Cebrian, E., Coma, R., Féral, J.P., La Rivière, M., Linares, C., López-Sendino, P., Marschal, C., Ribes, M., Teixidó, N., Zuberer, F., Garrabou, J., 2017. Regional and local environmental conditions do not shape the response to warming of a marine habitat-forming species. Sci. Rep. 7 (1), 5069. https://doi.org/10.1038/s41598-017-05220-4.

Dahlke, F.T., Leo, E., Mark, F.C., Pörtner, H.O., Bickmeyer, U., Frickenhaus, S., Storch, D., 2017. Effects of ocean acidification increase embryonic sensitivity to thermal extremes in Atlantic cod, *Gadus morhua*. Glob. Change Biol. 23 (4), 1499–1510. https://doi.org/10.1111/gcb.13527.

Davies, S.W., Marchetti, A., Ries, J.B., Castillo, K.D., 2016. Thermal and pCO_2 stress elicit divergent transcriptomic responses in a resilient coral. Front. Mar. Sci. 3, 112. https://doi.org/10.3389/fmars.2016.00112.

Diaz-Almela, E., Marbà, N., Duarte, C.M., 2007. Consequences of Mediterranean warming events in seagrass (*Posidonia oceanica*) flowering records. Glob. Chang. Biol. 13 (1), 224–235. https://doi.org/10.1111/j.1365-2486.2006.01260.x.

Guide to best practices for ocean CO_2 measurement. In: Dickson, A.G., Sabine, C.L., Christian, J.R. (Eds.), 2007. PICES Special Publication 3; IOCCP Report 8. North Pacific Marine Science Organization, Sidney, British Columbia. https://doi.org/10.25607/OBP-1342 (191 pp.).

Dimond, J.L., Roberts, S.B., 2016. Germline DNA methylation in reef corals: patterns and potential roles in response to environmental change. Mol. Ecol. 25 (8), 1895–1904. https://doi.org/10.1111/mec.13414.

Dixon, G., Bay, L.K., Matz, M.V., 2016. Evolutionary consequences of DNA methylation in a basal metazoan. Mol. Biol. Evol. 33 (9), 2285–2293. https://doi.org/10.1093/molbev/msw100.

Dixon, G., Liao, Y., Bay, L.K., Matz, M.V., 2018. Role of gene body methylation in acclimatization and adaptation in a basal metazoan. Proc. Natl. Acad. Sci. 115 (52), 13342–13346. https://doi.org/10.1073/pnas.1813749115.

Dixon, G., Matz, M., 2022. Changes in gene body methylation do not correlate with changes in gene expression in Anthozoa or Hexapoda. BMC Genom. 23 (1). https://doi.org/10.1186/s12864-022-08474-z.

Doney, S.C., Ruckelshaus, M., Emmett Duffy, J., Barry, J.P., Chan, F., English, C.A., Galindo, H.M., Grebmeier, J.M., Hollowed, A.B., Knowlton, N., Polovina, J., Rabalais, N.N., Sydeman, W.J., Talley, L.D., 2012. Climate change impacts on marine ecosystems. Ann. Rev. Mar. Sci. 4, 11–37. https://doi.org/10.1146/annurev-marine-041911-111611.

Doonan, L.B., Hartigan, A., Okamura, B., Long, P.F., 2019. Stress-free evolution: the Nrf-coordinated oxidative stress response in early diverging metazoans. Integr. Comp. Biol. 59 (4), 799–810. https://doi.org/10.1093/icb/icz055.

Dupont, S., Dorey, N., Stumpp, M., Melzner, F., Thorndyke, M., 2013. Long-term and trans-life-cycle effects of exposure to ocean acidification in the green sea urchin *Strongylocentrotus droebachiensis*. Mar. Biol. 160 (8), 1835–1843. https://doi.org/10.1007/s00227-012-1921-x.

Estaque, T., Richaume, J., Bianchimani, O., Schull, Q., Mérigot, B., Bensoussan, N., Bonhomme, P., Vouriot, P., Sartoretto, S., Monfort, T., Basthard-Bogain, S., Fargetton, M., Gatti, G., Barth, L., Cheminée, A., Garrabou, J., 2023. Marine heatwaves on the rise: one of the strongest ever observed mass mortality event in temperate gorgonians. Glob. Chang. Biol. 29 (22), 6159–6162. https://doi.org/10.1111/gcb.16931.

Ezzat, L., Merle, P.L., Furla, P., Buttler, A., Ferrier-Pages, C., 2013. The response of the Mediterranean gorgonian *Eunicella singularis* to thermal stress is independent of its nutritional regime. PloS One 8 (5), e64370. https://doi.org/10.1371/journal.pone.0064370.

Falfushynska, H.I., Wu, F., Ye, F., Kasianchuk, N., Dutta, J., Dobretsov, S., Sokolova, I.M., 2019. The effects of ZnO nanostructures of different morphology on bioenergetics and stress response biomarkers of the blue mussels *Mytilus edulis*. Sci. Total Environ. 694, 133717. https://doi.org/10.1016/j.scitotenv.2019.133717.

Feely, R.A., Alin, S.R., Newton, J., Sabine, C.L., Warner, M., Devol, A., Krembs, C., Maloy, C., 2010. The combined effects of ocean acidification, mixing, and respiration on pH and carbonate saturation in an urbanized estuary. Estuar. Coast. Shelf Sci. 88 (4), 442–449. https://doi.org/10.1016/j.ecss.2010.05.004.

Gammon, M.J., Tracey, D.M., Marriott, P.M., Cummings, V.J., Davy, S.K., 2018. The physiological response of the deep-sea coral *Solenosmilia variabilis* to ocean acidification. PeerJ 6, e5236. https://doi.org/10.7717/peerj.5236.

Garrabou, J., Coma, R., Bensoussan, N., Bally, M., Chevaldonné, P., Cigliano, M., Diaz, D., Harmelin, J.G., Gambi, M.C., Kersting, D.K., Ledoux, J.B., Lejeusne, C., Linares, C., Marschal, C., Pérez, T., Ribes, M., Romano, J.C., Serrano, E., Teixido, N., Torrents, O., Zabala, M., Zuberer, F., Cerrano, C., 2009. Mass mortality in Northwestern Mediterranean rocky benthic communities: effects of the 2003 heat wave. Glob. Chang. Biol. 15 (5), 1090–1103. https://doi.org/10.1111/j.1365-2486.2008.01823.x.

Garrabou, J., Gómez-Gras, D., Medrano, A., Cerrano, C., Ponti, M., Schlegel, R., Harmelin, J.G., 2022. Marine heatwaves drive recurrent mass mortalities in the Mediterranean Sea. Glob. Chang. Biol. 28 (19), 5708–5725. https://doi.org/10.1111/gcb.16301.

Gavery, M.R., Roberts, S.B., 2013. Predominant intragenic methylation is associated with gene expression characteristics in a bivalve mollusc. Peer J 1, e215. https://doi.org/10.6084/m9.figshare.749728.

Ge, S.X., Jung, D.M., Yao, R.A., 2020. ShinyGO: a graphical gene-set enrichment tool for animals and plants. Bioinformatics 36, 2628–2629. https://doi.org/10.1093/bioinformatics/btz931.

Gómez-Gras, D., Bensoussan, N., Ledoux, J.B., López-Sendino, P., Cerrano, C., Ferretti, E., Kipson, S., Garrabou, J., 2022. Exploring the response of a key Mediterranean gorgonian to heat stress across biological and spatial scales. Sci. Rep. 12 (1), 21064. https://doi.org/10.1038/s41598-022-25565-9.

Gönülal, O., 2021. Sea water temperature in the North Aegean Sea (Gökçeada Island) between 1972 and 2018: an implication of global warming. J. Black Sea/Mediterr. Environ. 27, 24–33.

Guerrero, L., Bay, R., 2024. Patterns of methylation and transcriptional plasticity during thermal acclimation in a reef-building coral. Evolutionary Applications 17 (7), e13757. https://doi.org/10.1111/eva.13757.

Haas, B.J., Papanicolaou, A., Yassour, M., Grabherr, M., Blood, P.D., Bowden, J., Couger, M.B., Eccles, D., Li, B., Lieber, M., MacManes, M.D., Ott, M., Orvis, J., Pochet, N., Strozzi, F., Weeks, N., Westerman, R., William, T., Dewey, C.N., Henschel, R., LeDuc, R.D., Friedman, N., Regev, A., 2013. De novo transcript sequence reconstruction from RNA-seq using the Trinity platform for reference generation and analysis. Nat. Protoc. 8, 1494–1512. https://doi.org/10.1038/nprot.2013.084.

Hackerott, S., Martell, H.A., Eirin-Lopez, J.M., 2021. Coral environmental memory: causes, mechanisms, and consequences for future reefs. Trends Ecol. Evol. 36 (11), 1011–1023. https://doi.org/10.1016/j.tree.2021.06.014.

Haider, F., Sokolov, E.P., Sokolova, I.M., 2018. Effects of mechanical disturbance and salinity stress on bioenergetics and burrowing behavior of the soft-shell clam *Mya arenaria*. J. Exp. Biol. 221 (4), jeb172643. https://doi.org/10.1242/jeb.172643.

Haslun, J.A., Hauff-Salas, B., Strychar, K.B., Ostrom, N.E., Cervino, J.M., 2018. Biotic stress contributes to seawater temperature induced stress in a site-specific manner for Porites astreoides. Mar. Biol. 165, 1–13. https://doi.org/10.1007/s00227-018-3414-z.

Hawes, N.A., Tremblay, L.A., Pochon, X., Dunphy, B., Fidler, A.E., Smith, K.F., 2018. Effects of temperature and salinity stress on DNA methylation in a highly invasive marine invertebrate, the colonial ascidian *Didemnum vexillum*. Peer J 6, e5003. https://doi.org/10.7717/peerj.5003.

Helton, E.S., Chen, X., 2007. p53 modulation of the DNA damage response. J. Cell. Biochem. 100 (4), 883–896. https://doi.org/10.1002/jcb.21091.

Hemond, E.M., Vollmer, S.V., 2015. Diurnal and nocturnal transcriptomic variation in the Caribbean staghorn coral, *Acropora cervicornis*. Mol. Ecol. 24 (17), 4460–4473. https://doi.org/10.1111/mec.13320.

Iborra, L., Leduc, M., Fullgrabe, L., Cuny, P., Gobert, S., 2022. Temporal trends of two iconic Mediterranean gorgonians (*Paramuricea clavata* and *Eunicella cavolini*) in the climate change context. J. Sea Res. 186, 102241. https://doi.org/10.1016/j.seares.2022.102241.

IPCC, 2021. Summary for policymakers. In: Masson-Delmotte, V., Zhai, P., Pirani, A., Connors, S.L., Péan, C., Berger, S., Caud, N., Chen, Y., Goldfarb, L., Gomis, M.I., Huang, M., Leitzell, K., Lonnoy, E., Matthews, J.B.R., Maycock, T.K., Waterfield, T., Yelekçi, O., Yu, R., Zhou, B. (Eds.), Climate Change 2021: The Physical Science Basis. Contribution of Working Group I to the Sixth Assessment Report of the Intergovernmental Panel on Climate Change. Cambridge University Press, Cambridge, United Kingdom and New York, NY, USA, pp. 3–32. https://doi.org/10.1017/9781009157896.001.

IPCC, 2022. Summary for policymakers [Pörtner, H.-O., Roberts, D.C., Poloczanska, E.S., Mintenbeck, K., Tignor, M., Alegría, A., Craig, M., Langsdorf, S., Löschke, S., Möller, V., Okem, A. (eds.)]. In: Climate Change 2022: Impacts, Adaptation, and Vulnerability. Contribution of Working Group II to the Sixth Assessment Report of the Intergovernmental Panel on Climate Change [Pörtner, H.-O., Roberts, D.C., Tignor, M., Poloczanska, E.S., Mintenbeck, K., Alegría, A., Craig, M., Langsdorf, S., Löschke, S., Möller, V., Okem, A., Rama, B. (eds.)]. Cambridge University Press, Cambridge, UK and New York, NY, USA, pp. 3–33. https://doi.org/10.1017/9781009325844.001.

Ishida-Castañeda, J., Iguchi, A., Sakai, K., 2023. Changes in DNA methylation in response to heat stress and symbiotic conditions in coral primary polyps. Mar. Ecol. Prog. Ser. 714, 113–117. https://doi.org/10.3354/meps14344.

Jia, S., Geng, X., Cai, Z., Wang, Y., Shen, J., Li, Y., Wang, D., 2024. Comparison of physiological and transcriptome responses of corals to strong light and high temperature. Ecotoxicol. Environ. Saf. 273, 116143. https://doi.org/10.1016/j.ecoenv.2024.116143.

Jiang, L., Sun, Y.F., Zhou, G.W., Tong, H.Y., Huang, L.T., Yu, X.L., Huang, H., 2022. Ocean acidification elicits differential bleaching and gene expression patterns in larval reef coral *Pocillopora damicornis* under heat stress. Sci. Total Environ. 842, 156851. https://doi.org/10.1016/j.scitotenv.2022.156851.

Jiang, L., Zhang, P., Huang, L.T., Yu, X.L., Liu, C.Y., Yuan, X.C., Liu, S., Huang, H., 2024. Life-stage specificity and temporal variations in transcriptomes and DNA methylomes of the reef coral *Pocillopora damicornis* in response to thermal acclimation. Sci. Total Environ., 171098 https://doi.org/10.1016/j.scitotenv.2024.171098.

Jurriaans, S., Hoogenboom, M.O., Ferrier-Pages, C., 2021. Similar thermal breadth of two temperate coral species from the Mediterranean Sea and two tropical coral species from the Great Barrier Reef. Coral Reefs 40 (4), 1281–1295. https://doi.org/10.1007/s00338-021-02139-1.

Kemena, C., Dohmen, E., Bornberg-Bauer, E., 2019. DOGMA: a web server for proteome and transcriptome quality assessment. Nucleic Acids Res. 47, W507–W510. https://doi.org/10.1093/nar/gkz366.

Khalil, M., Doo, S.S., Stuhr, M., Westphal, H., 2023. Long-term physiological responses to combined ocean acidification and warming show energetic trade-offs in an asterinid starfish. Coral Reefs 42 (4), 845–858. https://doi.org/10.1007/s00338-023-02388-2.

Lange, K., Maguer, J.F., Reynaud, S., Ferrier-Pagès, C., 2023. Nutritional ecology of temperate octocorals in a warming ocean. Front. Mar. Sci. 10. https://doi.org/10.3389/fmars.2023.1236164.

Ledoux, J.B., Cruz, F., Gómez-Garrido, J., Antoni, R., Blanc, J., Gómez-Gras, D., Kipson, S., López-Sendino, P., Antunes, A., Linares, C., Gut, M., Alioto, T., Garrabou, J., 2020. The genome sequence of the octocoral *Paramuricea clavata* - a key resource to study the impact of climate change in the Mediterranean. G3 (Bethesda, Md.) 10 (9), 2941–2952. https://doi.org/10.1534/g3.120.401371.

Lesser, M.P., Farrell, J.H., 2004. Exposure to solar radiation increases damage to both host tissues and algal symbionts of corals during thermal stress. Coral Reefs 23, 367–377. https://doi.org/10.1007/s00338-004-0392-z.

Leung, J.Y.S., Zhang, S., Connell, S.D., 2022. Is ocean acidification really a threat to marine calcifiers? A systematic review and meta-analysis of 980+ studies spanning two decades. Small 18, 2107407. https://doi.org/10.1002/smll.202107407.

Li, J., Long, L., Zou, Y., Zhang, S., 2021. Microbial community and transcriptional responses to increased temperatures in coral *Pocillopora damicornis* holobiont. Environ. Microbiol. 23 (2), 826–843. https://doi.org/10.1111/1462-2920.15168.

Liew, Y.J., Zoccola, D., Li, Y., Tambutté, E., Venn, A.A., Michell, C.T., Cui, G., Deutekom, E.S., Kaandorp, J.A., Voolstra, C.R., Forét, S., Allemand, D., Tambutté, S., Aranda, M., 2018. Epigenome-associated phenotypic acclimatization to ocean acidification in a reef-building coral. Sci. Adv. 4 (6), eaar8028. https://doi.org/10.1126/sciadv.aar8028.

Macleod, K.L., Paris, J.R., Jenkins, T.L., Stevens, J.R., 2023. The first genome of the cold-water octocoral, the pink sea fan, *Eunicella verrucosa*. Genome Biol. Evol. 15 (6), evad083. https://doi.org/10.1093/gbe/evad083.

Masuko, T., Minami, A., Iwasaki, N., Majima, T., Nishimura, S.I., Lee, Y.C., 2005. Carbohydrate analysis by a phenol–sulfuric acid method in microplate format. Anal. Biochem. 339 (1), 69–72. https://doi.org/10.1016/j.ab.2004.12.001.

McCauley, M., Banaszak, A.T., Goulet, T.L., 2018. Species traits dictate seasonal-dependent responses of octocoral–algal symbioses to elevated temperature and ultraviolet radiation. Coral Reefs 37, 901–917. https://doi.org/10.1007/s00338-018-1716-8.

MEDECC, 2024. Summary for policymakers. In: Djoundourian, S., Lionello, P., Llasat, M. C., Guiot, J., Cramer, W., Driouech, F., Gattacceca, J.C., Marini, K. (Eds.), Climate and Environmental Coastal Risks in the Mediterranean, MedECC Reports. MedECC Secretariat, Marseille, France, ISBN 978-2-493662-03-3, p. 28. https://doi.org/10.5281/zenodo.10722133.

Melzner, F., Thomsen, J., Koeve, W., Oschlies, A., Gutowska, M.A., Bange, H.W., Hansen, H.P., Steinhoff, T., Körtzinger, A., 2013. Future ocean acidification will be amplified by hypoxia in coastal habitats. Mar. Biol. 160, 1875–1888. https://doi.org/10.1007/s00227-012-1954-1.

Miao, Z., Xu, D., Cui, M., Zhang, Q., 2016. High mobility group protein DSP1 negatively regulates HSP70 transcription in *Crassostrea hongkongensis*. Biochem. Biophys. Res. Commun. 474 (4), 634–639. https://doi.org/10.1016/j.bbrc.2016.03.163.

Mirdita, M., Steinegger, M., Soding, J., 2019. MMseqs2 desktop and local web server app for fast, interactive sequence searches. Bioinformatics 35, 2856–2858. https://doi.org/10.1093/bioinformatics/bty1057.

Mukherjee, K., Moroz, L.L., 2024. Parallel evolution of transcription factors in basal metazoans. In: Ctenophores: Methods and Protocols. Springer US, New York, NY, pp. 491–508. https://doi.org/10.1007/978-1-0716-3642-8_20.

Negishi, H., Taniguchi, T., Yanai, H., 2018. The interferon (IFN) class of cytokines and the IFN regulatory factor (IRF) transcription factor family. Cold Spring Harb. Perspect. Biol. 10 (11), a028423. https://doi.org/10.1101/cshperspect.a028423.

Nishimura, O., Hara, Y., Kuraku, S., 2017. gVolante for standardizing completeness assessment of genome and transcriptome assemblies. Bioinformatics 33, 3635–3637. https://doi.org/10.1093/bioinformatics/btx445.

Orenes-Salazar, V., Navarro-Martínez, P.C., Ruíz, J.M., García-Charton, J.A., 2023. Recurrent marine heatwaves threaten the resilience and viability of a key Mediterranean octocoral species. Aquat. Conserv. Mar. Freshwat. Ecosyst. 33 (11), 1161–1174. https://doi.org/10.1002/aqc.3997.

Özalp, H.B., Alparslan, M., 2016. Scleractinian diversity in the Dardanelles and Marmara Sea (Turkey): morphology, ecology and distributional patterns. Oceanol. Hydrobiol. Stud. 45 (2), 259–285. https://doi.org/10.1515/ohs-2016-0023.

Pappalardo, X.G., Barra, V., 2021. Losing DNA methylation at repetitive elements and breaking bad. Epigenetics Chromatin 14 (1), 25. https://doi.org/10.1186/s13072-021-00400-z.

Pereira, S.M.D.C., 2019. Thermotolerance Experiments and Transplantation Procedures of Four Gorgonian Species From the South Coast of Portugal, Algarve. http://hdl.handle.net/10400.1/13520.

Pey, A., Zamoum, T., Allemand, D., Furla, P., Merle, P.L., 2011. Depth-dependant thermotolerance of the symbiotic Mediterranean gorgonian *Eunicella singularis*: evidence from cellular stress markers. J. Exp. Mar. Biol. Ecol. 404 (1–2), 73–78. https://doi.org/10.1016/j.jembe.2011.05.007.

Pey, A., Catanéo, J., Forcioli, D., Merle, P.L., Furla, P., 2013. Thermal threshold and sensitivity of the only symbiotic Mediterranean gorgonian *Eunicella singularis* by morphometric and genotypic analyses. C. R. Biol. 336 (7), 331–341. https://doi.org/10.1016/j.crvi.2013.06.008.

Pivotto, I.D., Nerini, D., Masmoudi, M., Kara, H., Chaoui, L., Aurelle, D., 2015. Highly contrasted responses of Mediterranean octocorals to climate change along a depth gradient. R. Soc. Open Sci. 2 (5), 140493. https://doi.org/10.1098/rsos.140493.

Pörtner, H.O., 2008. Ecosystem effects of ocean acidification in times of ocean warming: a physiologist's view. Mar. Ecol. Prog. Ser. 373, 203–217. https://doi.org/10.3354/meps07768.

Pörtner, H.O., Langenbuch, M., Reipschläger, A., 2004. Biological impact of elevated ocean CO_2 concentrations: lessons from animal physiology and earth history. J. Oceanogr. 60, 705–718. https://doi.org/10.1007/s10872-004-5763-0.

Previati, M., Scinto, A., Cerrano, C., Osinga, R., 2010. Oxygen consumption in Mediterranean octocorals under different temperatures. J. Exp. Mar. Biol. Ecol. 390 (1), 39–48. https://doi.org/10.1016/j.jembe.2010.04.025.

Putnam, H.M., 2021. Avenues of reef-building coral acclimatization in response to rapid environmental change. J. Exp. Biol. 224 (Suppl_1), jeb239319. https://doi.org/10.1242/jeb.239319.

Putnam, H.M., Davidson, J.M., Gates, R.D., 2016. Ocean acidification influences host DNA methylation and phenotypic plasticity in environmentally susceptible corals. Evol. Appl. 9 (9), 1165–1178. https://doi.org/10.1111/eva.12408.

R Studio Team, 2021. Integrated Development Environment for R. http://www.rstudio.com/.

Raghavan, V., Eichele, G., Larink, O., Karin, E.L., Soding, J., 2023. RNA sequencing indicates widespread conservation of circadian clocks in marine zooplankton. NAR Genom Bioinform 5, lqad007. https://doi.org/10.1093/nargab/lqad007.

Rivetti, I., Fraschetti, S., Lionello, P., Zambianchi, E., Boero, F., 2014. Global warming and mass mortalities of benthic invertebrates in the Mediterranean Sea. PloS One 9 (12), e115655. https://doi.org/10.1371/journal.pone.0115655.

Rodolfo-Metalpa, R., Martin, S., Ferrier-Pagès, C., Gattuso, J.P., 2010. Response of the temperate coral Cladocora caespitosa to mid-and long-term exposure to pCO_2 and temperature levels projected for the year 2100 AD. Biogeosciences 7 (1), 289–300. https://doi.org/10.5194/bgd-6-7103-2009.

Rodrigues, L.J., Grottoli, A.G., 2007. Energy reserves and metabolism as indicators of coral recovery from bleaching. Limnol. Oceanogr. 52 (5), 1874–1882. https://doi.org/10.4319/lo.2007.52.5.1874.

Rosa, R., Rummer, J.L., Munday, P.L., 2017. Biological responses of sharks to ocean acidification. Biol. Lett. 13 (3), 20160796. https://doi.org/10.1098/rsbl.2016.0796.

Rossi, S., Gili, J.M., Coma, R., Linares, C., Gori, A., Vert, N., 2006. Temporal variation in protein, carbohydrate, and lipid concentrations in *Paramuricea clavata* (Anthozoa, Octocorallia): evidence for summer–autumn feeding constraints. Mar. Biol. 149, 643–651. https://doi.org/10.1007/s00227-005-0229-5.

Savary, R., Barshis, D.J., Voolstra, C.R., Cárdenas, A., Evensen, N.R., Banc-Prandi, G., Meibom, A., 2021. Fast and pervasive transcriptomic resilience and acclimation of extremely heat-tolerant coral holobionts from the northern Red Sea. Proc. Natl. Acad. Sci. 118 (19), e2023298118. https://doi.org/10.1073/pnas.2023298118.

Sebé-Pedrós, A., de Mendoza, A., 2015. Transcription factors and the origin of animal multicellularity. In: Evolutionary Transitions to Multicellular Life: Principles and Mechanisms, pp. 379–394. https://doi.org/10.1007/978-94-017-9642-2_18.

Shirur, K.P., Ramsby, B.D., Iglesias-Prieto, R., Goulet, T.L., 2014. Biochemical composition of Caribbean gorgonians: implications for gorgonian—Symbiodinium symbiosis and ecology. J. Exp. Mar. Biol. Ecol. 461, 275–285. https://doi.org/10.1016/j.jembe.2014.08.016.

Sokolova, I., 2021. Bioenergetics in environmental adaptation and stress tolerance of aquatic ectotherms: linking physiology and ecology in a multi-stressor landscape. J. Exp. Biol. 224 (Suppl_1), jeb236802. https://doi.org/10.1242/jeb.236802.

Tignat-Perrier, R., van de Water, J.A., Guillemain, D., Aurelle, D., Allemand, D., Ferrier-Pagès, C., 2022. The effect of thermal stress on the physiology and bacterial communities of two key Mediterranean gorgonians. Appl. Environ. Microbiol. 88 (6). https://doi.org/10.1128/aem.02340-21 (e02340-21).

Tom, M., Douek, J., Yankelevich, I., Bosch, T.C., Rinkevich, B., 1999. Molecular characterization of the first heat shock protein 70 from a reef coral. Biochem. Biophys. Res. Commun. 262 (1), 103–108.

UniProt, 2023. The universal protein knowledgebase in 2023. Nucleic Acids Res. 51 (D1), D523–D531.

Van Handel, E., 1985. Rapid determination of total lipids in mosquitoes. J. Am. Mosq. Control Assoc. 1 (3), 302–304.

Vargas, C.A., Lagos, N.A., Lardies, M.A., Duarte, C., Manríquez, P.H., Aguilera, V.M., Broitman, B., Widdicombe, S., Dupont, S., 2017. Species-specific responses to ocean acidification should account for local adaptation and adaptive plasticity. Nature Ecology & Evolution 1 (4), 0084. https://doi.org/10.1038/s41559-017-0084.

Vargas, C.A., Cuevas, L.A., Broitman, B.R., San Martin, V.A., Lagos, N.A., Gaitán-Espitia, J.D., Dupont, S., 2022. Upper environmental pCO_2 drives sensitivity to ocean acidification in marine invertebrates. Nat. Clim. Chang. 12 (2), 200–207. https://doi.org/10.1038/s41558-021-01269-2.

Walling, L.K., 2020. Phylogenetic and Depth Effects on Whole Genome DNA Methylation in Octocorallia. University of Louisiana at Lafayette (ProQuest Dissertations & Theses, 28030853).

Wood, D.E., Lu, J., Langmead, B., 2019. Improved metagenomic analysis with Kraken 2. Genome Biol. 20, 1–13. https://doi.org/10.1186/s13059-019-1891-0.

Wu, H., Li, J., Song, Q., Chai, G., Xiao, Y., Li, Z., 2023. The synergistic negative effects of combined acidification and warming on the coral host and its symbiotic association with Symbiodiniaceae indicated by RNA-Seq differential expression analysis. Coral Reefs 42 (5), 1187–1201. https://doi.org/10.1007/s00338-023-02425-0.